

# Application of a Bayesian model to infer the contribution of coalbed natural gas produced water to the Powder River, Wyoming and Montana

Jason M. Mailloux,<sup>1,4</sup> Kiona Ogle<sup>2,3,5</sup> and Carol D. Frost<sup>1\*</sup>

<sup>1</sup> Department of Geology and Geophysics, University of Wyoming, Laramie, Wyoming, 82071, USA

<sup>2</sup> Department of Botany, University of Wyoming, Laramie, Wyoming, 82071, USA

<sup>3</sup> Department of Statistics, University of Wyoming, Laramie, Wyoming, 82071, USA

<sup>4</sup> ConocoPhillips, 600 North Dairy Ashford Road, Houston, Texas, 77079, USA

<sup>5</sup> School of Life Sciences, Arizona State University, Tempe, Arizona, 85287, USA

## Abstract:

The Powder River Basin (PRB) of Wyoming and Montana contains significant coal and coal bed natural gas (CBNG) resources. CBNG extraction requires the production of large volumes of water, much of which is discharged into existing drainages. Compared to surface waters, the CBNG produced water is high in sodium relative to calcium and magnesium, elevating the sodium adsorption ratio (SAR). To mitigate the possible impact this produced water may have on the quality of surface water used for irrigation, the State of Montana passed water anti-degradation legislation, which could affect CBNG production in Wyoming.

In this study, we sought to determine the proportion of CBNG produced water discharged to tributaries that reaches the Powder River by implementing a four end-member mixing model within a Bayesian statistical framework. The model accounts for the  $^{87}\text{Sr}/^{86}\text{Sr}$ ,  $\delta^{13}\text{C}_{\text{DIC}}$ , [Sr] and [DIC] of CBNG produced water and surface water interacting with the three primary lithologies exposed in the PRB. The model estimates the relative contribution of the end members to the river water, while incorporating uncertainty associated with measurement and process error.

Model results confirm that both of the tributaries associated with high CBNG activity are mostly composed of CBNG produced water (70–100%). The model indicates that up to 50% of the Powder River is composed of CBNG produced water downstream from the CBNG tributaries, decreasing with distance by dilution from non-CBNG impacted tributaries from the point sources to ~10–20% at the Montana border. This amount of CBNG produced water does not significantly affect the SAR or electrical conductivity of the Powder River in Montana. Copyright © 2013 John Wiley & Sons, Ltd.

KEY WORDS carbon isotopes;  $\delta^{13}\text{C}$ ; coal bed natural gas; dissolved inorganic carbon; strontium isotopes;  $^{87}\text{Sr}/^{86}\text{Sr}$ ; isotope mixing model; sodium adsorption ratio; water pollution

Received 8 August 2011; Accepted 19 February 2013

## INTRODUCTION

The Powder River Basin (PRB) is an asymmetrical structural and sedimentary north-northwest-trending Tertiary basin that encompasses 55 962 km<sup>2</sup> (~21 600 mi<sup>2</sup>), extending from northeastern Wyoming into southeastern Montana (Figure 1) (Flores and Bader, 1999). The coal seams in the basin occur in the Paleocene Fort Union Formation and the overlying Eocene Wasatch Formation (Flores and Bader, 1999). The basin boundaries are defined by the Bighorn Mountains on the west, the Black Hills on the east, the Laramie Mountains on the south and the Miles City Arch on the north. The PRB has a semi-arid climate, receiving an average of 30–35 cm of precipitation annually (Sharp and Gibbons, 1964).

Approximately 25% of the coal reserves in the United States are contained within the subbituminous and bituminous

coal seams in the PRB that have an average thickness of ~7.5 m (~25 ft) (Ayers *et al.*, 1984). The methane in these seams is trapped in micropores as a free gas, in coal cleats as a dissolved gas in water within the coal, as an adsorbed gas on the surface of the macerals that comprise the coal or as an adsorbed gas within the structure of the bulk coal (DeBruin *et al.*, 2004). The coal bed natural gas (CBNG) produced in the PRB accounts for about 1.4% of the total amount of natural gas produced in the United States (WOGCC, 2012).

The number of CBNG wells in Wyoming has increased dramatically, from just 152 in 1995 to over 18 000 wells in 2008, but decreased to ~13 500 producing wells by the end of 2011 (Wyoming Oil and Gas Conservation Commission (WOGCC), 2012). In order to produce CBNG, the hydrostatic pressure of the coal seams is reduced by pumping water out of the coal seams to the surface to decrease the pressure in the coal seam, allowing the methane to rise through the wellbore to the surface. The wells in the PRB produce an average of ~11 700 l (~3080 gallons) of water per well per day (WOGCC, 2012), and over 7 trillion liters (~1.85 trillion gallons) of water are predicted to be produced over the lifetime

\*Correspondence to: Carol D. Frost, Department of Geology and Geophysics, University of Wyoming, 1000 E. University Ave., Laramie, Wyoming 82071, USA  
E-mail: frost@uwyo.edu

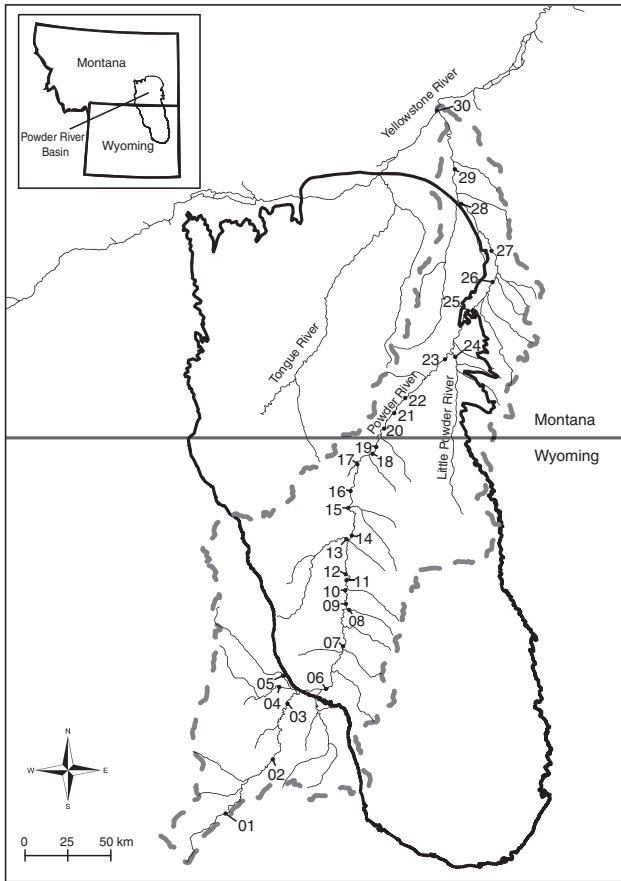


Figure 1. Map indicating the location of the Powder River Basin (dark outline), the Powder River watershed (dashed line) and numbered sampling locations

development of the PRB (~45 years at present production rates) (DeBruin *et al.*, 2004). This water is commonly disposed of by dispersing it over the land surface as irrigation, discharging to existing drainages, dispersed into the air by sprayers, or diverting it to off-channel holding ponds.

CBNG produced water is high in sodium relative to calcium and magnesium, particularly in wells located near the Powder River along the Johnson-Campbell county line in Wyoming (Campbell *et al.*, 2008). This is of particular importance because the ratio of sodium ( $\text{Na}^+$ ) to calcium ( $\text{Ca}^{2+}$ ) and magnesium ( $\text{Mg}^{2+}$ ), known as the sodium adsorption ratio (SAR), is an indication of the suitability of water for irrigation. When units are in milliequivalents per liter, the equation for SAR is given by (Stumm and Morgan, 1996):

$$\text{SAR} = \frac{[\text{Na}^+]}{\sqrt{\frac{[\text{Ca}^{2+}] + [\text{Mg}^{2+}]}{2}}} \quad (1)$$

When using SAR as an anti-degradation index, it is important to note that linear mixing models do not work for SAR because of the square root term in the denominator. The ionic concentrations of two waters mixing must be known in order to accurately calculate the SAR of the mixed water. Total dissolved solids (TDS) also can be high in

produced water, reaching over 3000 mg/l in the central area of the PRB (Campbell *et al.*, 2008). Thus, the addition of produced water—particularly water produced from wells in the central portion of the PRB in Wyoming—has the potential to significantly increase the SAR and TDS of surface waters.

The Powder River originates in Wyoming and flows north into Montana. It is approximately 500 km long and has a highly variable discharge (Figure 2). The discharge over the duration of this study was as low as  $0.085 \text{ m}^3 \text{ s}^{-1}$  ( $\sim 3 \text{ ft}^3 \text{ s}^{-1}$ ) at the low-flow periods and over  $100 \text{ m}^3 \text{ s}^{-1}$  ( $\sim 3500 \text{ ft}^3 \text{ s}^{-1}$ ) during high flow associated with spring melt (Figure 3) (United States Geological Survey (USGS) (2010)). The quality of this water is of particular concern because it is used for irrigation and may be affected by inputs from CBNG produced water. In 2003 and 2006, the State of Montana promulgated regulations to address potential water quality impacts of CBNG development on agriculture in the Tongue and Powder rivers of northeastern Wyoming and southeastern Montana. According to these rules, which the United States Environmental Protection Agency (EPA) approved in 2003 and 2008, the monthly average electrical conductivity (EC; a field measurement that serves as a proxy for TDS) during the irrigation season must not exceed  $2000 \mu\text{S}/\text{cm}$  with no sample above  $2500 \mu\text{S}/\text{cm}$ , and the monthly average SAR must not be above 5 with no sample exceeding 7.5 (Montana Department of Environmental Quality, 2006). By these rules, if the surface water flowing from Wyoming to Montana does not meet these standards, then Wyoming may have to limit its CBNG production or modify its water management strategies until a solution can be determined to lower the SAR and EC of this water. The Montana standards were challenged, and in 2009, the US District Court, District of Wyoming, remanded the matter to EPA to consider whether the numeric standards are based upon appropriate technical and scientific data (Pennaco, 2009). During the EPA’s reconsideration of the standards on

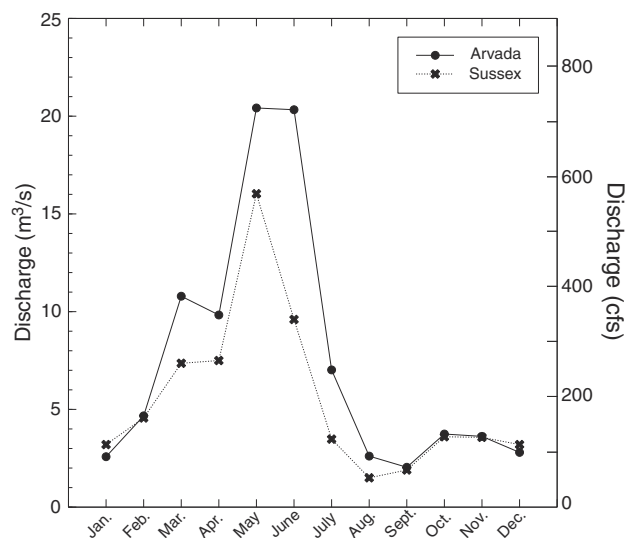


Figure 2. Powder River average monthly discharge from 1930 to 2008 for USGS gauging stations at Arvada and Sussex, Wyoming. Data from United States Geological Survey (USGS) National Water Information System (2010)

COAL BED NATURAL GAS PRODUCED WATER IN THE POWDER RIVER

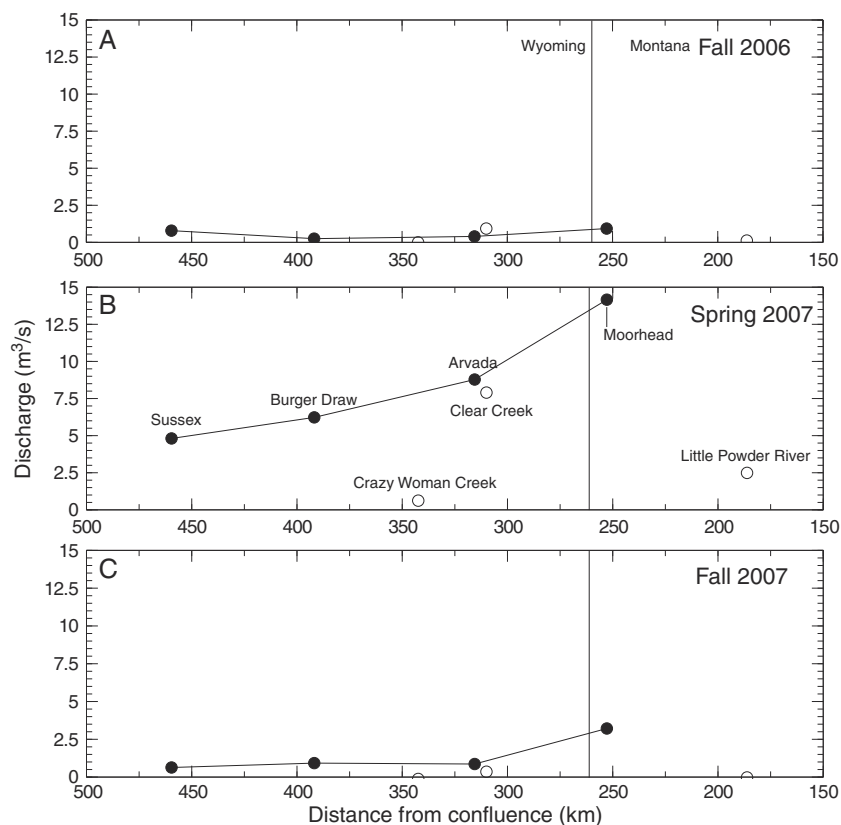


Figure 3. Powder River discharge at the time of sampling. Tributaries are denoted by open symbols. (a) Low-flow period (22 September 2006), (b) high-flow period (2 May 2007) and (c) low-flow period (1 September 2007). The horizontal grey line indicates the location of the Wyoming-Montana boarder. Data are from United States Geological Survey (USGS) National Water Information System (2010)

remand, the Montana Board of Environmental Review initiated a review of Montana’s water quality standards and determined that the existing standards are necessary to protect water quality and soils (Compton, 2011).

The goal of this study was to determine the proportional contribution of CBNG produced water to the Powder River and evaluate the impact of CBNG activity on SAR and EC. This information will help to establish future standards for water in the Powder River. Because of the paucity of gauging stations on the Powder River (five stations; Clark *et al.*, 2005), uncertainties in water volumes carried by tributaries, and conveyance loss in holding ponds and infiltration, simple volumetric calculations to determine the proportion of CBNG produced water are not possible. The few studies that have been conducted to evaluate how much infiltration and conveyance loss occurs from the impoundments and ponds that hold CBNG produced water have shown that these quantities are very difficult to estimate, in part because they are temporally (seasonally) dynamic (Brink and Frost, 2007; Payne and Saffer, 2005; Wheaton and Brown, 2005). Two studies, however, examined historical water quality data from the Powder River to determine whether there were changes that may be attributed to development of CBNG activity in the PRB. Clark and Mason (2007) could not establish a causal link with gas production and instead established that streamflow was the strongest control on water quality. Statistical analysis of historical water quality data by Wang *et al.* (2007), by contrast, did identify changes in water quality.

These changes were attributed to CBNG development without considering other explanations, such as the decade-long drought that coincided with the development of CBNG in Wyoming.

Conventional linear mixing models could potentially be applied to  $\delta^{18}\text{O}$  and  $\delta^2\text{H}$  to infer the contribution of CBNG produced water, but the use of  $\delta^{18}\text{O}$ ,  $\delta^2\text{H}$ , and major ions pose several challenges. For example, the relevant  $\delta^{18}\text{O}$  and  $\delta^2\text{H}$  end members are difficult to define (see Figure 4) due to seasonal variation and evaporative enrichment effects. Likewise, most major ions are similar in concentration in both CBNG produced water and Powder River water (i.e. iron, sodium and TDS; Figure 5) and thus cannot be utilized for mixing models. For other ions, such as  $\text{Cl}^-$ , the concentration in CBNG produced water is low (~15 ppm) compared to Powder River water (~100–500 ppm) making the contribution of CBNG produced water impossible to distinguish from natural variations in surface water (Figure 5).

The hydrology of the PRB is also very complex and adds to the difficulty in tracing CBNG produced water. The Tertiary units in the PRB that affect the hydrology are the Wasatch Formation and the Fort Union Formation (composed of the Tongue River Formation, the Lebo Shale Member and the Tullock Member (Hinaman, 2005); Figure 6). Hotchkiss and Levings (1986) discuss the complexities of the shallow hydrogeology in the PRB, emphasizing the sparse potentiometric data in the area and hydrologic communication between the Tertiary

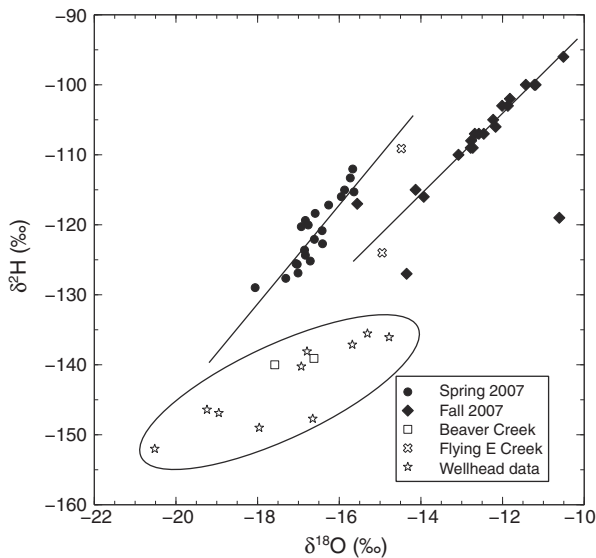


Figure 4.  $\delta^2\text{H}$  versus  $\delta^{18}\text{O}$  for the Powder River. Powder River data are from Carter (2008). Wellhead data are from Campbell (2007)

formations in the region making it difficult to fully characterize the ground water flow paths in the region. They conclude that ‘the major sources of recharge to the shallow hydrogeologic units are infiltration of water from precipitation and streamflow on areas of outcrop. Infiltration from losing streams is also a component of recharge.’ The fact that the Powder River is a losing stream further complicates volumetric calculations and reinforces the

need for distinct environmental tracers to better understand the fate of CBNG produced water in the PRB.

In summary, conventional linear mixing models cannot be used with confidence in combination with  $\delta^{18}\text{O}$ ,  $\delta^2\text{H}$  or ionic tracers to estimate the proportional contribution of CBNG produced water in the Powder River. Thus, we address this problem through the application of mass-balance-based mixing models applied to strontium and carbon isotope and concentration measurements. The mixing models are implemented within a Bayesian statistical modeling framework to estimate the contribution of CBNG produced water to the Powder River during different seasons and flow conditions to capture the potential maximum and minimum effect of CBNG produced water on the Powder River. The Bayesian framework allows us to incorporate some constraints into the mixing model based on our knowledge of the lithology and hydrology of the PRB, and it also accommodates and explicitly estimates uncertainties in the end members and the relative contributions.

Strontium (Sr) is a useful hydrological tracer because, unlike hydrogen, oxygen and carbon, its isotopes do not fractionate measurably in nature. The  $^{87}\text{Sr}/^{86}\text{Sr}$  ratio provides a measure of the relative proportion of radiogenic to primordial strontium in a particular sample. Ground water obtains strontium from dissolution of minerals or ion-exchange reactions on mineral and rock surfaces (Frost *et al.*, 2002). Thus, the  $^{87}\text{Sr}/^{86}\text{Sr}$  ratio represents a time-integrated record of rock–water interactions. Differences in

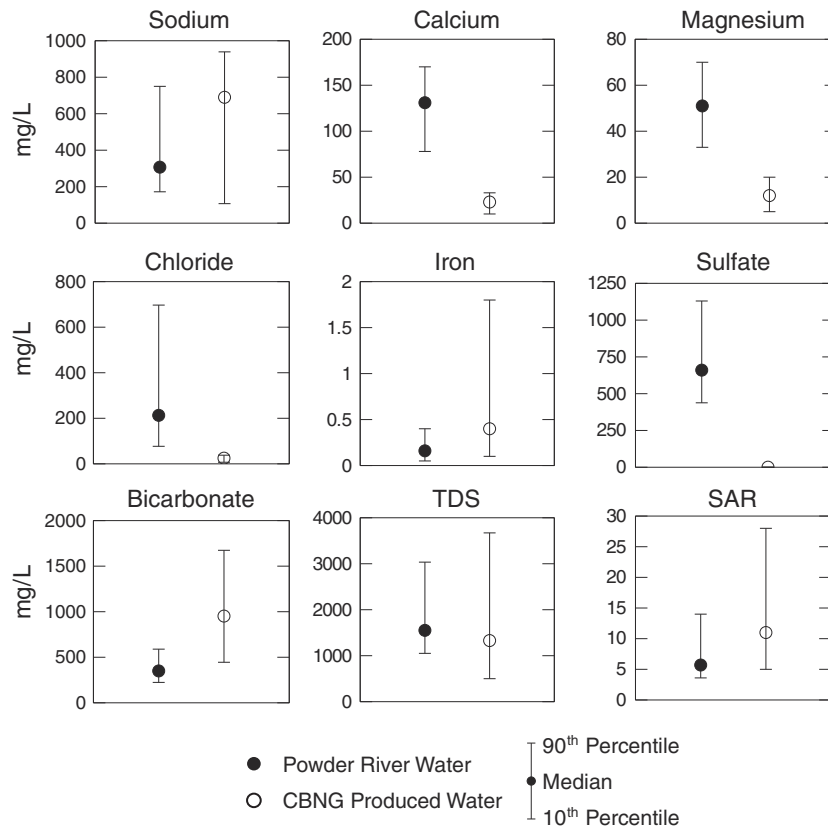


Figure 5. Major ion chemistry for the Powder River (closed circles) and CBNG produced water (open circles). Circles represent the median value; black bars represent the range between the 10<sup>th</sup> and 90<sup>th</sup> percentiles. TDS = total dissolved solids. Powder River data are from United States Geological Survey (USGS) National Water Information System (2010), and CBNG data are from Campbell *et al.* (2008), Pearson (2002) and Quillinan and Frost (2012)

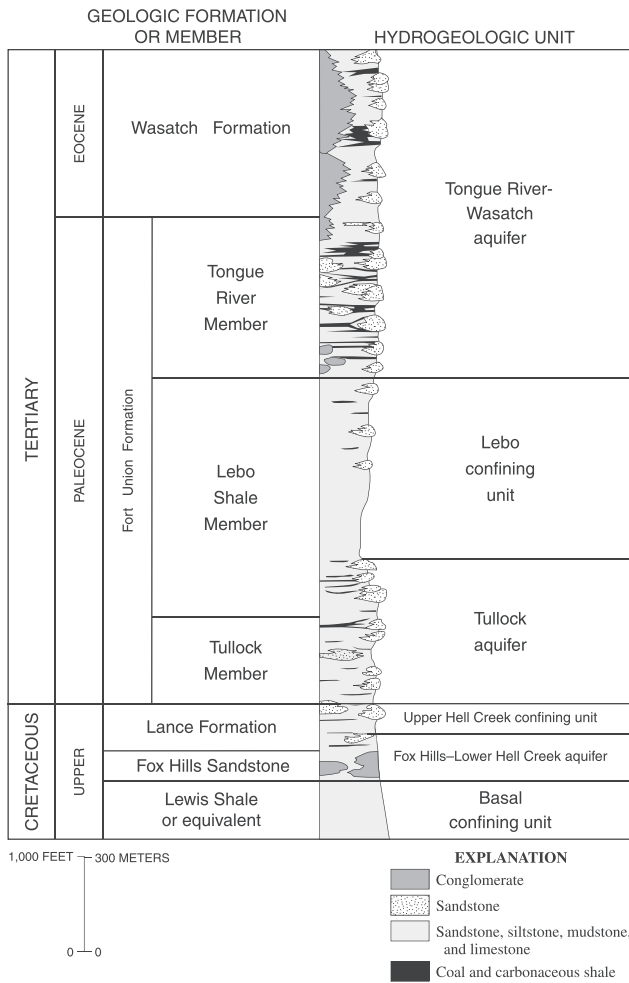


Figure 6. Generalized stratigraphic column of Tertiary and upper Cretaceous formations in the southern Powder River structural basin, Wyoming (from Hinaman, 2005)

the  $^{87}\text{Sr}/^{86}\text{Sr}$  ratio in water indicate natural variations of this ratio in geologic materials. Measurements of the  $^{87}\text{Sr}/^{86}\text{Sr}$  ratio are extremely precise ( $\pm 0.00001$ ), allowing very small differences in ground water composition to be detected (Frost *et al.*, 2002). This precision allows the  $^{87}\text{Sr}/^{86}\text{Sr}$  ratio to be a valuable and effective tool to trace the effects of CBNG production in the PRB. For example, the  $^{87}\text{Sr}/^{86}\text{Sr}$  ratio of the CBNG waters is more radiogenic and more variable ( $^{87}\text{Sr}/^{86}\text{Sr} = 0.71268$  to  $0.71510$ ) than the  $^{87}\text{Sr}/^{86}\text{Sr}$  ratio from sandstone aquifers ( $0.71258$  to  $0.71271$ ) (Brinck and Frost, 2007; Campbell *et al.*, 2008; Frost *et al.*, 2002). The  $^{87}\text{Sr}/^{86}\text{Sr}$  ratio in Powder River water ( $^{87}\text{Sr}/^{86}\text{Sr} = 0.70817$  to  $0.71968$ ) represents a mixture of water sources, with one of the potentially important sources being CBNG produced water. Strontium concentration ( $[\text{Sr}]$ ) is primarily used for mass-balance considerations in the Bayesian mixing model. The strontium concentration typically ranges from 0 to 3 mg/l in the water sources examined in this study. This small range of values makes it difficult to fingerprint each water source using only  $[\text{Sr}]$ , but in combination with the  $^{87}\text{Sr}/^{86}\text{Sr}$  ratio, we can determine the proportional contribution of each water source to a mixture as long as we have a reasonable estimate of the end-member values of each source.

Sharma and Frost (2008) also suggest that the dissolved inorganic carbon concentration ( $[\text{DIC}]$ ) and the  $^{13}\text{C}/^{12}\text{C}$  ratio measured in the DIC ( $\delta^{13}\text{C}_{\text{DIC}}$ ) can be used to monitor CBNG produced water infiltration into ground water and streams. Produced waters associated with CBNG have a strongly positive  $\delta^{13}\text{C}_{\text{DIC}}$  ( $12\text{‰}$  to  $22\text{‰}$ ), which is easily distinguishable from the negative  $\delta^{13}\text{C}_{\text{DIC}}$  value of most surface and ground water ( $-11\text{‰}$  to  $-8\text{‰}$ ) (Whiticar, 1999). Additionally,  $[\text{DIC}]$  in produced water is elevated ( $>100$  mg C/l) compared to other ground and surface waters (20 to 50 mg C/l) in the PRB (Sharma and Frost, 2008). The  $\delta^{13}\text{C}$  composition of carbon sources and sinks is the controlling factor of the  $\delta^{13}\text{C}_{\text{DIC}}$  of natural waters. Carbon dioxide ( $\text{CO}_2$ ) derived from microbial decay of organic matter and root respiration are the two major sources of carbon contributing to DIC in natural waters, while atmospheric  $\text{CO}_2$  is negligible (Mook and Tan, 1991). The elevated  $\delta^{13}\text{C}_{\text{DIC}}$  and  $[\text{DIC}]$  in CBNG produced water can be explained by the preferential removal of  $^{12}\text{C}$  by bacteria in an organic-rich system during microbial methanogenesis. The preferential removal of the isotopically lighter molecules during methanogenesis (resulting in the release of isotopically light  $\text{CH}_4$ ) results in a progressive shift in the remaining carbon pool towards heavier,  $^{13}\text{C}$ -enriched values (Whiticar, 1999). These processes create distinct end members that allow for partitioning of CBNG *versus* natural waters in the Powder River.

We simultaneously fit mass-balance-based mixing models to  $^{87}\text{Sr}/^{86}\text{Sr}$  ratio,  $[\text{Sr}]$ ,  $\delta^{13}\text{C}_{\text{DIC}}$  and  $[\text{DIC}]$  data that were collected along the Powder River to infer the contribution of CBNG produced water. To accommodate these data sources and complexities associated with the missing model, we implemented the analysis within a Bayesian framework. Bayesian statistical methods for fitting process models (e.g. mixing models) to data (e.g. isotope ratios and concentrations) have been used successfully to trace particular water sources in hydrology (Cable *et al.*, 2011; Hong *et al.*, 2005), and we adopt this approach for several reasons. First, a Bayesian framework was selected because of its ability to accommodate multiple isotopic and concentration data sources (Cable *et al.*, 2011; Ogle *et al.*, 2004), handle missing data (Cable *et al.*, 2009; Gelman *et al.*, 2004; Gelman and Hill, 2006), model uncertainty in measurements and strontium and carbon end members (Cable *et al.*, 2011), and incorporate other (e.g. prior or published) sources of information (Gelman *et al.*, 2004) as well as deal with temporal or seasonal variations in the data (Cable *et al.*, 2008). Second, the Bayesian approach also allows for the explicit modeling of different sources of error such as analytical (or instrument) error and additional 'observation' (or sampling) error (Ogle and Barber, 2008). The ability to handle missing data is particularly useful because the data set for fall 2006 is incomplete, but the data that was collected can still be used in the model in conjunction with the full data sets of spring 2007 and fall 2007 to estimate the proportional contribution of CBNG produced water as well as to help constrain end-member estimates for all field seasons. We implemented a mixing model in a Bayesian framework (e.g. Moore and Semmens,

2008; Parnell *et al.*, 2010; Cable *et al.*, 2011) to infer the contributions of CBNG produced water *versus* surface water (i.e. the water in the Powder River not contributed by produced water, regardless of source), the ionic composition and isotopic composition of which we allowed to vary by lithology traversed. Both strontium and carbon isotopes and concentrations are simultaneously utilized within a Bayesian framework to estimate these contributions. The analysis produces probabilistic-based estimates (e.g. Moore and Semmens, 2008) of the contribution of CBNG produced water to the Powder River.

## FIELD AND LABORATORY METHODS

Water samples were collected at 30 locations along the Powder River (Figure 1, Table I). The first five sample locations (PR01–PR05) were along the North, Middle and South Forks of the Powder River. Sample site PR06 is the first site along the main reach of the Powder River after the confluence of the three forks. Included among the sample stations are several tributaries farther downstream: PR08 on Beaver Creek, PR11 on Flying E Creek, PR13 on Crazy Woman Creek and PR24 on the Little Powder River. Sample sites PR01–PR07 are upstream of CBNG

Table I. Powder River Basin sample locations. See Figure 1 for a map of the locations (UTM datum WGS 84)

Sample site	Distance from confluence (km)	Northing	Easting (Zone 13)
PR01	591.3	4766322	336181
PR02	539.3	4798277	363776
PR03	489.8	4830723	372814
PR04	493.6	4840581	368156
PR05	493.6	4847136	370425
PR06	459.6	4838986	395490
PR07	426.2	4863584	405029
PR08 <sup>a</sup>	395.1	4885374	409426
PR09	391.8	4888353	408967
PR10	381.2	4896333	407674
PR11 <sup>a</sup>	373.1	4903285	408353
PR12	366.8	4905668	407693
PR13 <sup>a</sup>	342.4	4926418	409454
PR14	337.9	4928245	411128
PR15	315.6	4944614	410392
PR16	304.7	4954444	411981
PR17	284.9	4970095	416088
PR18	271.8	4975957	424995
PR19	266.5	4980082	427294
PR20	252.8	4990855	431479
PR21	240.1	4999069	438621
PR22	227.3	5007747	445415
PR23	189.6	5030649	468337
PR24 <sup>a</sup>	186.2	5034180	468337
PR25	154.9	5066509	493260
PR26	123.8	5075452	496210
PR27	100.9	5093222	495917
PR28	64.8	5121381	479662
PR29	42.6	5141577	476170
PR30	0.0	5176001	467182

<sup>a</sup> Tributary

activity, whereas sample sites PR08–PR19 are all within the zone of CBNG production (USGS, 2005).

River water samples were collected at each of the sites in each of three field seasons: fall of 2006 (21–24 September 2006), spring of 2007 (31 May–3 June 2007) and fall of 2007 (31 August–3 September 2007). These times were selected to span the greatest variance in water volume (i.e. high flow *vs* low flow) to determine if there was seasonal variability in the amount of CBNG produced water reaching the Powder River. The fall 2006 sampling season was marred by heavy rain, causing some roads to be impassable and resulted in incomplete sampling of the Powder River, but yielding data pertaining to a storm event (Table II). Spring 2007 represents a true high-flow state (as high as  $\sim 100 \text{ m}^3 \text{ s}^{-1}$ ) during the spring melt, and fall 2007 represents a true low-flow state (as low as  $0.085 \text{ m}^3 \text{ s}^{-1}$ ) of the river.

River water was collected and filtered using 0.45 micron filters and kept cold and dark until analysis. Acidified and untreated 60 ml aliquots were used for major cation and anion analysis, respectively. Major ions were analyzed by atomic absorption, ion chromatography, inductively coupled plasma-mass spectrometry and acid–base titration procedures. Errors associated with major ion concentration measurements typically range between  $\pm 3\%$  and  $5\%$ . A 3 ml aliquot of each untreated sample was then evaporated, redissolved in 3.5 M  $\text{HNO}_3$  and passed through Teflon columns filled with Eichrom<sup>®</sup> Sr-Spec resin to isolate strontium and analyzed for  $^{87}\text{Sr}/^{86}\text{Sr}$  by thermal ionization mass spectrometry on a VG Sector at the University of Wyoming Radiogenic Isotope Laboratory. Standard reproducibility was  $0.71025 \pm 0.00005$  (two standard deviations), based on 15 analyses of the NBS987 standard.

Samples collected for  $\delta^{13}\text{C}_{\text{DIC}}$  and [DIC] were passed through a  $0.45 \mu\text{m}$  filter. Two to three drops of benzalkonium were added to each sample to halt any metabolic activity. Samples were analyzed for  $\delta^{13}\text{C}_{\text{DIC}}$  using a GasBench-II device coupled to a Finnegan DELTA plus mass spectrometer in the Stable Isotope Facility at the University of Wyoming. The reproducibility and accuracy, as monitored by replicate analysis of samples and internal lab standards, were better than  $\pm 0.1\%$ . The  $\delta^{13}\text{C}_{\text{DIC}}$  values are reported in per mil relative to the carbon isotope standard Vienna Pee Dee belemnite. DIC concentrations were determined by acid–base titrations as described in Sharma and Frost (2008). The relative standard uncertainty of the DIC concentration measurement in this study was  $\pm 3\%$ .

## BAYESIAN MIXING MODEL

A mass-balance-based mixing was developed and implemented in a Bayesian framework to estimate the relative contributions of four different sources in a four end-member mixing model. The sources that we considered were: CBNG produced water and three surface water sources based on lithology, including precipitation that

Table II. Strontium and carbon isotopic and concentration data. NA indicates missing data

Sample site	Fall 2006				Spring 2007				Fall 2007			
	87Sr/86Sr	Sr (ppm)	δ13CDIC	DIC (mg C/l)	87Sr/86Sr	Sr (ppm)	δ13CDIC	DIC (mg C/l)	87Sr/86Sr	Sr (ppm)	δ13CDIC	DIC (mg C/l)
PR 01	0.71309	0.21	-10.90	NA	0.71097	1.95	-10.03	NA	0.71284	0.19	-16.86	NA
PR 02	0.71836	1.53	-11.40	NA	0.71904	3.26	-9.78	33	0.71968	3.00	-8.73	NA
PR 03	0.71367	2.17	-8.30	NA	0.71264	2.90	-7.59	31	0.71196	2.78	-8.57	NA
PR 04	0.70906	1.20	-9.50	NA	0.70958	0.47	-8.68	33	0.70954	1.15	-9.03	NA
PR 05	0.71109	1.09	-10.60	NA	0.71065	1.06	-10.38	38	0.71086	0.92	-11.71	NA
PR 06	0.71385	2.29	-4.70	NA	0.71108	1.22	-8.33	41	0.71338	2.63	-1.03	NA
PR 07	0.71290	1.98	-1.40	NA	0.71134	1.38	-6.77	45	0.71155	2.09	-4.58	NA
PR 08	0.71335	0.44	16.40	NA	0.71288	0.70	15.84	253	0.71344	0.27	17.35	NA
PR 09	0.71284	1.81	5.40	NA	0.71122	1.25	1.17	65	0.71186	1.72	2.85	NA
PR 10	0.71287	1.52	NA	NA	0.71134	1.20	0.64	NA	0.71187	1.77	3.55	NA
PR 11	0.70995	0.35	13.70	NA	0.71292	0.25	12.63	106	0.71027	0.12	14.44	NA
PR 12	0.71254	1.67	9.60	NA	0.71138	1.25	2.1	65	0.71172	1.74	4.11	NA
PR 13	NA	NA	NA	NA	0.71035	0.85	-8.2	NA	0.71113	1.29	-5.28	NA
PR 14	0.71166	0.68	13.00	NA	0.71138	1.07	0.08	54	0.71172	1.74	2.74	NA
PR 15	0.71174	0.99	9.50	NA	0.71137	1.10	0	51	0.71165	1.55	2.41	NA
PR 16	NA	NA	NA	NA	0.71141	1.15	-0.2	NA	0.71160	1.47	2.62	NA
PR 17	NA	NA	NA	NA	0.71139	1.27	-1.24	NA	0.71151	1.51	-0.43	NA
PR 18	NA	NA	NA	NA	0.71128	0.90	-3.12	NA	0.71144	1.35	-0.48	NA
PR 19	NA	NA	NA	NA	0.71126	0.95	-3.27	NA	0.71146	1.42	-0.53	NA
PR 20	NA	NA	NA	NA	0.71124	1.00	-3.65	NA	0.71135	1.49	0.51	NA
PR 21	NA	NA	NA	NA	0.71122	1.03	-4.24	NA	0.71129	1.62	1.14	NA
PR 22	NA	NA	NA	NA	0.71118	0.94	-4.37	NA	0.71122	1.31	0.74	NA
PR 23	0.71109	1.40	-5.60	NA	0.71120	1.03	-3.52	43	0.71102	1.50	-3.17	NA
PR 24	0.71001	1.40	-8.90	NA	0.71093	1.89	-10.18	77	0.71067	1.27	-10.28	NA
PR 25	NA	NA	NA	NA	0.71118	1.18	-4.69	NA	0.71082	1.73	-4.98	NA
PR 26	NA	NA	NA	NA	0.71086	1.13	-4.83	NA	0.71080	1.80	-5.42	NA
PR 27	NA	NA	NA	NA	0.71084	1.24	-5.54	NA	0.71071	1.59	-6.3	NA
PR 28	NA	NA	NA	NA	0.71068	1.03	-6.04	NA	0.71080	1.52	-6.28	NA
PR 29	0.70847	0.18	-9.70	NA	0.71045	0.87	-6.63	41	0.71078	1.60	-5.82	NA
PR 30	0.70817	0.24	-9.50	NA	0.71045	0.91	-6.32	42	0.71067	1.65	-5.00	NA

reached the river via overland flow that traversed these lithologies and water that infiltrated through the lithologies and reached river via subsurface flow: (1) carbonate rocks, (2) Tertiary shales and sandstones and (3) Archean gneisses and granites. Because differences in the  $^{87}\text{Sr}/^{86}\text{Sr}$  ratios among these sources typically occur in the third or fourth decimal place, the measured  $^{87}\text{Sr}/^{86}\text{Sr}$  value for each sample was multiplied by 1000 for ease in data handling and analysis. This rescaling does not affect the mass-balance assumption of the mixing models since all samples and end members were rescaled. The  $\delta^{13}\text{C}_{\text{DIC}}$ , [Sr] and [DIC] data were not rescaled.

Direct inputs of rainwater are assumed to be a negligible component of this system because the PRB generally receives little precipitation input (30–35 cm annually), and precipitation is low in strontium (typically 0.0 to 0.5 ppm) (Clow *et al.*, 1997; Frost and Toner, 2004). Any rainwater that falls directly into the Powder River is of an inconsequential volume when considered in relation to the PRB as a whole. The vast majority of the rain that falls in the Powder River watershed that reaches the river will reach it by overland flow; this water will not have the ‘rainwater’ signature, but will carry the signature of the local exchangeable salts and silica from the soil, thus having a strontium signal that more closely represents the local lithology (i.e. one of the surface water end members).

#### Likelihood of isotope ratio and concentration data

The Bayesian isotope mixing model that we constructed has three different components that define the likelihoods of observed  $^{87}\text{Sr}/^{86}\text{Sr}$ ,  $\delta^{13}\text{C}_{\text{DIC}}$ , [Sr] and [DIC] data. The first is used to estimate the three surface water end members based on the isotope ratio and concentration data collected upstream of the Beaver Creek confluence. The second is used to estimate the CBNG end-member values based on measurements made along Beaver Creek, a tributary of the Powder River that is known to contain large amounts of CBNG produced water (Wyoming Department of Environmental Quality (WDEQ), 2006, 2008). Beaver Creek water is known to represent CBNG produced water because the Sr and C isotopic composition of Beaver Creek water is within the range of  $^{87}\text{Sr}/^{86}\text{Sr}$  ratios and  $\delta^{13}\text{C}_{\text{DIC}}$  of CBNG-produced water collected directly from wellheads (Frost *et al.*, 2002; Brinck and Frost, 2007; Sharma and Frost, 2008). The third incorporates a four end-member mixing model to determine the contributions of the four different sources (i.e. CBNG water and the three surface waters) to water in the Powder River occurring downstream of the Beaver Creek confluence, and in Flying E Creek, another tributary downstream of Beaver Creek that also contains CBNG produced water. Each of these components involves parameters that we wish to estimate such as the ‘true’ end-member signatures, the relative contributions of each end member (or source), a parameter that indicates how quickly the CBNG signature dissipates (with respect to distance from Beaver Creek and Flying E Creek) and any variance terms related to measurement error or process error.

The process error represents uncertainty introduced by our simplification of the processes leading to the observed  $^{87}\text{Sr}/^{86}\text{Sr}$ ,  $\delta^{13}\text{C}_{\text{DIC}}$ , [Sr] and [DIC] in the river water.

The  $\delta^{13}\text{C}_{\text{DIC}}$  and [DIC] components of the system are separated into two end members. Although there is significant end-member variability in the DIC system, it can be best defined by a natural water component ( $\delta^{13}\text{C}_{\text{DIC}} = -11\text{‰}$  to  $-8\text{‰}$  and [DIC] = 20 to 50 mg C/l) and a CBNG component ( $\delta^{13}\text{C}_{\text{DIC}} = 12\text{‰}$  to  $22\text{‰}$  and [DIC] > 100 mg C/l) rather than defined by lithology.

The surface water end members are based on data collected from the headwaters of the Powder River (the South, Middle and North Forks) and are defined by the sample sites that are south (upstream) of current CBNG activity (WOGCC, 2012). In addition to field data (Table II), end member  $^{87}\text{Sr}/^{86}\text{Sr}$ ,  $\delta^{13}\text{C}_{\text{DIC}}$ , [Sr] and [DIC] information was obtained from the literature for areas near the study area (Frost *et al.*, 2006; Frost and Toner, 2004; Sharma and Frost, 2008); a unique aspect of the Bayesian approach is that it allows us to incorporate this information in the form of prior distributions (below). The literature-derived prior information and the isotope and concentration data collected for this study helped to determine the range of possible values for each end member.

The CBNG end member is based on data collected from Beaver Creek, which is composed almost entirely of CBNG produced water. Between 150 and 180 CBNG wells discharge their produced water into Beaver Creek, up to ~10.75 million liters per day (2.84 million gallons per day (Mgal/d) or  $4.39 \text{ ft}^3 \text{ s}^{-1}$ ) (WDEQ, 2006), which represents more than 90% of the approximately  $0.057 \text{ m}^3 \text{ s}^{-1}$  ( $\sim 2 \text{ ft}^3 \text{ s}^{-1}$ ) for Beaver Creek that is recorded year round (USGS, 2010). Flying E Creek also receives CBNG produced water inputs (WOGCC, 2012), currently 0.3 million liters of produced water per day (0.08 Mgal/d;  $0.12 \text{ ft}^3 \text{ s}^{-1}$ ), but is permitted to carry up to 9.46 million liters of produced water per day (2.5 Mgal/d;  $3.9 \text{ ft}^3 \text{ s}^{-1}$ ) (WDEQ, 2008). We account for this in the model by allowing for CBNG inputs at both Beaver Creek and Flying E Creek. We report the proportion of CBNG produced water in the Powder River as the sum of the CBNG contributed via Beaver Creek and via Flying E Creek. Additionally, CBNG wellhead data were used to determine the possible range of values for the CBNG end member (Campbell *et al.*, 2008; Sharma and Frost, 2008).

In specifying the Bayesian mixing model, we first define the likelihood of all  $^{87}\text{Sr}/^{86}\text{Sr}$ ,  $\delta^{13}\text{C}_{\text{DIC}}$ , [Sr] and [DIC] data. We assume that these quantities are normally distributed with mean values ( $\mu$ ) given by the ‘true’  $^{87}\text{Sr}/^{86}\text{Sr}$ ,  $\delta^{13}\text{C}_{\text{DIC}}$ , [Sr] and [DIC] values ( $\mu_X$ ) of these waters, and variance ( $\sigma_X^2$ ) that reflects temporal variability introduced by the measurement and sampling processes (where data set  $X = ^{87}\text{Sr}/^{86}\text{Sr}$ ,  $\delta^{13}\text{C}_{\text{DIC}}$ , [Sr] or [DIC]). For field season  $j$  ( $j = 1, 2$  or  $3$ , where  $1 = \text{fall } 2006$ ,  $2 = \text{spring } 2007$  and  $3 = \text{fall } 2007$ ) and sampling location  $i$  ( $i = 1, 2, \dots, 30$ ) along the Powder River, we assume the following general form for the isotopic and elemental concentration distributions:

$$X_{i,j} \sim Normal(\mu_{X,i,j}, \sigma_X^2) \quad (2)$$

Equation (2) applies to the end-member data (i.e. based on the sampling locations upstream of Beaver Creek,  $i = 1-5$ , and from Beaver Creek,  $i = 8$ ), the Powder River ‘mixture’ data (i.e. samples collected from locations  $i = 6, 7, 9-30$ ), and the Flying E Creek ‘mixture’ data (i.e. location  $i = 11$ ). Locations 6 and 7 are assumed to be a mixture of only the natural water sources as these locations occur downstream of the confluence of the three forks of the Powder River, but upstream of Beaver Creek and Flying E Creek; locations 9–30 occur downstream of the CBNG inputs associated with Beaver Creek.

*The end member and mixing models*

Next, we develop ‘process’ models to define the means ( $\mu$ ) in the likelihood in Equation (3). The definition of the means depends on whether a sampling location was used to estimate an end member or reflects a mixture of the end members. In particular, for  $X = {}^{87}\text{Sr}/{}^{86}\text{Sr}$  or  $[\text{Sr}]$  and for  $X' = \delta^{13}\text{C}_{\text{DIC}}$  or  $[\text{DIC}]$  (we only consider two end members), we define  $\mu_{X,i,j}$  as:

$$\mu_{X,i,j} = \begin{cases} \mu_{X,arc} & \text{for } i = 1, 2, 3 \\ \mu_{X,carb} & \text{for } i = 4 \\ \mu_{X,tert} & \text{for } i = 5 \\ \mu_{X,cbng} & \text{for } i = 8 \\ \mu_{X,mix,i,j} & \text{for } i = 6, 7, 9, 10, \dots, 30 \end{cases} \quad (3)$$

$$\mu_{X',i,j} = \begin{cases} \mu_{X',sur} & \text{for } i = 1, 2, \dots, 5 \\ \mu_{X',cbng} & \text{for } i = 8 \\ \mu_{X',mix,i,j} & \text{for } i = 6, 7, 9, 10, \dots, 30 \end{cases}$$

Where  $\mu_{X,arc}$ ,  $\mu_{X,carb}$  and  $\mu_{X,tert}$  represent the mean values for the three surface water end members, which reflect water interactions with Archean gneisses and granites, carbonate rocks, and Tertiary shale and sandstone, respectively;  $\mu_{X,sur}$

The relative contributions of CBNG water and water interacting with Archean-, carbonate- and Tertiary rocks vary by station ( $i$ ) and season ( $j$ ) and are given by  $p_{cbng}$ ,  $p_{arc}$ ,  $p_{carb}$  and  $p_{tert}$ , respectively. Equation (4) is specified such that  $p_{arc}$ ,  $p_{carb}$  and  $p_{tert}$  are the contributions of the surface waters relative to the other surface waters, such that  $p_{arc} + p_{carb} + p_{tert} = 1$ . Thus, when these contributions are multiplied by  $(1 - p_{cbng})$ , the overall contribution of the surface waters, this gives the relative contribution of each surface water when considering both surface and CBNG sources. For example, if Archean-derived surface waters account for 10% of the total surface contribution ( $p_{arc} = 0.10$ ), and if CBNG produced waters account for 30% of the total water ( $p_{cbng} = 0.30$ ), then Archean-derived waters account for an overall 7% ( $0.01 \times 0.70$ ) of the total water contribution. Note that the contributions of the surface waters, relative to only the surface waters, do not explicitly change with location  $i$ . However, once they are adjusted for the CBNG contribution ( $1 - p_{cbng}$ ), the relative contribution of the surface waters compared to CBNG changes because  $p_{cbng}$  depends on location in the Powder River, as defined in Equation (5). Note that Equation (4) is a fairly standard mixing model that obeys mass-balance constraints.

Only sample sites PR08 to PR10 ( $i = 8, 9, 10$ ) are modeled with Beaver Creek as the only CBNG produced water input. Station PR11 ( $i = 11$ ), Flying E Creek, is a tributary of the Powder River and is assumed to be partly composed of CBNG water. The remaining stations (PR12–PR30,  $i = 12, 13, \dots, 30$ ) include CBNG inputs from both Beaver Creek and Flying E Creek. Thus, we modeled the contribution of CBNG water ( $p_{cbng}$ ) as an exponential function of distance from these two CBNG tributaries to reflect that dilution of the CBNG water as distance from these tributaries increases:

$$p_{cbng,i,j} = \begin{cases} p_{BC,j} \exp(-k_j \cdot D_{BC,i}) & i = 9, 10 \\ p_{FE,j}^0 & i = 11 \\ p_{BC,j} \exp(-k_j \cdot D_{BC,i}) + p_{FE,j} \exp(-k_j \cdot D_{FE,i}) & i = 12, 13, \dots, 30 \end{cases} \quad (5)$$

represents the mean end-member value for all surface water sources combined. The CBNG end-member mean value is represented by  $\mu_{X,cbng}$ , and  $\mu_{X,mix}$  is the mean given by a mixture of the surface and CBNG end-member values.

For  $X$  and  $X'$  as defined above, we define the mean for water collected at stations  $i = 6, 7, 9, 10, \dots, 30$  as the mixture of the four (for strontium) or two (for carbon) different end members:

$$\mu_{X,mix,i,j} = p_{cbng,i,j} \mu_{X,cbng} + (1 - p_{cbng,i,j}) \cdot (p_{arc,i,j} \mu_{X,arc} + p_{carb,i,j} \mu_{X,carb} + p_{tert,i,j} \mu_{X,tert}) \quad (4)$$

$$\mu_{X',mix,i,j} = p_{cbng,i,j} \mu_{X',cbng} + (1 - p_{cbng,i,j}) \cdot \mu_{X',sur}$$

Where  $p_{BC,j}$  is the initial contribution of CBNG produced water at the confluence of Beaver Creek, and the Powder River ( $D_{BC,8} = 0$ );  $p_{FE,j}^0$  is the initial contribution of CBNG water in Flying E Creek;  $D_{BC,i}$  and  $D_{FE,i}$  are the distances from Beaver Creek to station  $i$  ( $i = 8, 9, \dots, 30$ ) and from Flying E Creek to station  $i$  ( $i = 11, 12, \dots, 30$ ), respectively; and  $k$  is a source-specific decay constant to account for dilution and removal of strontium and carbon from the river. We assume that the dilution and removal process is independent of location such that  $k$  only varies by season. The need to account for dilution is indicated by the fact that Clear Creek, which enters the Powder River north of Arvada and south of the Montana border, has

approximately the same discharge as the Powder River above its confluence with Clear Creek (Figure 3) (USGS, 2010). Clear Creek carries dilute water from the Bighorn Mountains and receives little to no CBNG produced water. Note that Equation (5) applies the following restrictions to the contribution of CBNG produced water:  $0 \leq p_{cbng} \leq p_{BC}$  ( $i=9, 10$ ),  $0 \leq p_{cbng} \leq p_{FE}^0$  ( $i=11$ ), and  $0 \leq p_{cbng} \leq p_{BC} + p_{FE}$  ( $i=12, \dots, 30$ ).

*Priors and posterior*

The above Equations (1)–(5) combine to form a non-linear mixed effects model, which could theoretically be implemented in maximum likelihood framework. However, implementation via a Bayesian approach is more straightforward, especially given issues of missing data, multiple data sources and the desire to incorporate information from the literature. In the above models,  $p_{arc}$ ,  $p_{carb}$ ,  $p_{tert}$ ,  $p_{BC}$ ,  $p_{FE}$ ,  $p_{FE}^0$  and  $k$  are unknown parameters that we wish to estimate, and we define the parameter model (i.e. prior distributions) in this section. To complete the Bayesian model, we assigned normal priors to the end-member means, represented by  $\mu_{X,cbng}$ ,  $\mu_{X,arc}$ ,  $\mu_{X,carb}$  and  $\mu_{X,tert}$  (see Equation 6). That is, for the end members  $EM=arc, carb, tert$  or  $cbng$  and for  $X=^{87}\text{Sr}/^{86}\text{Sr}$ ,  $\delta^{13}\text{C}_{\text{DIC}}$ , [Sr] or [DIC]:

$$\mu_{X,EM} \sim \text{Normal}(\tilde{\mu}_{X,EM}, \tilde{\sigma}_{X,EM}^2) \quad (6)$$

A unique aspect of the Bayesian approach is the ability to incorporate prior information, and we took advantage of this by specifying slightly informative priors for some of the end members based on data available from the literature; use of such existing information is expected to help constrain the end members. Specifically, the values for  $\tilde{\mu}_{X,EM}$  and  $\tilde{\sigma}_{X,EM}^2$  for the surface and CBNG end members were based on isotope and concentration data from CBNG wellheads and Powder River water analyses (Clow *et al.*, 1997; Frost *et al.*, 2006; Frost and Toner,

2004; Sharma and Frost, 2008). See Table III for values used for  $\tilde{\mu}_{X,EM}$  and  $\tilde{\sigma}_{X,EM}^2$ . The likelihoods in Equation (6) also involve the variance terms ( $\sigma_X^2$ ), and we assigned standard (conjugate), non-informative gamma priors to the associated precision (1/variance) terms such that  $\sigma_X^{-2} \sim \text{Gamma}(0.1, 0.1)$  (Gelman *et al.*, 2004).

Note that the relative contributions ( $p$ 's) in Equation (4) are the same for all four data types ( $^{87}\text{Sr}/^{86}\text{Sr}$ , [Sr],  $\delta^{13}\text{C}_{\text{DIC}}$  or [DIC]). Further, to obey mass-balance constraints, we constrain the natural water  $p$ 's to be between zero and one and to sum to one for each station  $i$  and season  $j$  (i.e.  $1 = p_{arc,i,j} + p_{carb,i,j} + p_{tert,i,j}$ ). Thus, to achieve these constraints, we used a cumulative logits model for each natural water contribution term, relative to all surface waters ( $p_{arc}, p_{carb}, p_{tert}$ ) (Ogle *et al.*, 2006). We assigned non-informative priors to the remaining contribution or proportion parameters ( $p_{cbng}, p_{BC}, p_{FE}$  and  $p_{FE}^0$ ) by specifying diffuse normal priors (large variance) on the logit scale, where  $\text{logit}(p) = \log(p/(1-p))$ , obeying the constraint that  $0 \leq p \leq 1$ :

$$\begin{aligned} &\text{logit}(p_{cbng}), \text{logit}(p_{BC}), \text{logit}(p_{FE}), \quad (7) \\ &\text{logit}(p_{FE}^0) \sim \text{Normal}(0.0, 1000) \end{aligned}$$

Finally, we assigned a uniform (flat) prior to  $k$  on the interval (0, 1) such that  $k \sim \text{Uniform}(0,1)$ . A  $k$  value of zero indicates no dilution or removal of CBNG water, and a value of one indicates rapid loss of CBNG signature (e.g. via dilution, loss to infiltration, or affected by other processes to the extent that it is too small to detect) before reaching the next station downstream of Beaver Creek or Flying E Creek. It is highly unlikely that  $k$  would take on a value close to 1, and thus, the  $\text{Uniform}(0,1)$  prior is non-informative because it covers all possible values of  $k$ , including potentially unrealistic values.

Combining the likelihood and prior models within the Bayesian framework produces posterior distributions of all unknown quantities, where the posterior is propor-

Table III. End-member prior and posterior statistics (means and 2.5th and 97.5th percentiles) Note that  $^{87}\text{Sr}/^{86}\text{Sr}$  is the scaled value for each end member (=1000  $^{87}\text{Sr}/^{86}\text{Sr}$ )

End member	Prior mean	Prior 2.5%	Prior 97.5%	Post mean	Post. 2.5%	Post. 97.5%	Units	Post. Comparison*
[Sr] CBNG	0.5	0.05	2.6	0.5546	0.04734	1.258	mg/l	a
[Sr] Tertiary	1	0	2.9	1.021	0.2506	1.781	mg/l	a
[Sr] Archean	2	0	3.9	1.997	1.545	2.447	amg/l	b
[Sr] carbonate	0.5	0	2.7	0.9374	0.1781	1.707	mg/l	a
$^{87}\text{Sr}/^{86}\text{Sr}$ CBNG	713.2	707	719.5	713.2	711.6	714.9	unitless	a
$^{87}\text{Sr}/^{86}\text{Sr}$ Tertiary	711	709	712.9	710.9	709.7	712.2	unitless	b
$^{87}\text{Sr}/^{86}\text{Sr}$ Archean	713	711.1	715	714.4	713.5	715.2	unitless	c
$^{87}\text{Sr}/^{86}\text{Sr}$ carbonate	709	707	710.9	709.2	707.9	710.5	unitless	d
$\delta^{13}\text{C}_{\text{DIC}}$ CBNG	17.5	11.4	23.9	16.91	12.96	20.81	unitless	a
$\delta^{13}\text{C}_{\text{DIC}}$ Natural water	-10	-16.3	-3.9	-10.12	-12.29	-7.958	unitless	b
[DIC] CBNG	150	88.1	212.3	210.7	155.7	253.4	mg/l	a
[DIC] Natural Water	30	23.7	36.2	30.27	24.25	36.21	mg/l	b

\*Within each of the end-member type ([Sr],  $^{87}\text{Sr}/^{86}\text{Sr}$ ,  $\delta^{13}\text{C}$ , and [DIC]), posterior comparison indicates if the estimated end members are statistically different at the 5% level. Two quantities are considered statistically different if the posterior mean for one is not contained in the 95% CI for the other, and vice versa.

tional to the likelihood (of all data) multiplied by the priors (Gelman *et al.*, 2004; Ogle and Barber, 2008). That is, the posterior describes our updated understanding about each quantity given the data. Of particular interest are the posteriors for the end-member mean values and the relative contributions of the end members (sources) to the Powder River. We approximated the joint posterior of all unknown quantities by implementing the above model in WinBUGS, a free software package for conducting Bayesian analyses (Lunn *et al.*, 2000). Numerical sampling from the posterior was achieved by running three parallel Markov chain Monte Carlo (MCMC) chains; we evaluated the chains for convergence using the built-in convergence diagnostic tool ('bgr' tool) based on Gelman and Rubin (1992) and Brooks and Gelman (1998). Following standard procedures (Gilks *et al.*, 1996; Gelman *et al.*, 2004), we also evaluated the chains for a burn-in period (i.e. period prior to convergence) and discarded values associated with the burn-in (all chains converged by iteration 4000). The MCMC chains (posterior samples) were also evaluated for within chain autocorrelation, and chains were thinned every 10th iteration to obtain a relatively independent sample from the posterior. The model was run for 100 000 iterations, and posterior summary statistics were computed for 9600 samples post burn-in and thinning; that is, we computed posterior means and 95% credible intervals (2.5<sup>th</sup> and 97.5<sup>th</sup> percentiles) for each quantity of interest. Within the WinBUGS model, replicated data were created to evaluate model goodness-of-fit (Gelman *et al.*, 2004).

## RESULTS

Before presenting the posterior results, we note that the Bayesian mixing model fit the data sufficiently well (Figure 7). The model was fairly successful at capturing the strontium and carbon isotope ratio data (Figure 7a and 7c), but it was somewhat less successful at describing the concentration data, that is, the [Sr] and sparse [DIC] data (Figure 7b and 7d). The three most radiogenic measurements of  $^{87}\text{Sr}/^{86}\text{Sr}$  (Figure 7a) are also associated with the highest [Sr] values (three outliers in Figure 7b) and are from sample site PR02 on the South Fork of the Powder River. These ratios lie outside the 95% credible interval (CI) for the Archean end member (see Table III). The Bayesian model had trouble resolving extreme outliers such as these because of limitations in the data or assumptions about the potential sources. The model was, however, able to reproduce data associated with isotope values that were within the end-member values (Table III).

The Tertiary and carbonate end members have overlapping 95% CIs for  $^{87}\text{Sr}/^{86}\text{Sr}$  (Table III), which was not unexpected because these lithologies are commonly reported to have similar  $^{87}\text{Sr}/^{86}\text{Sr}$  values (Frost *et al.*, 2006; Frost and Toner, 2004). However, the 95% CIs for these end members do not contain each other's posterior means, and thus they are statistically different. In fact, all four end members are statistically different from each other when considering their  $^{87}\text{Sr}/^{86}\text{Sr}$  values (Table III). The end members show less separation in terms of [Sr] (Table III);

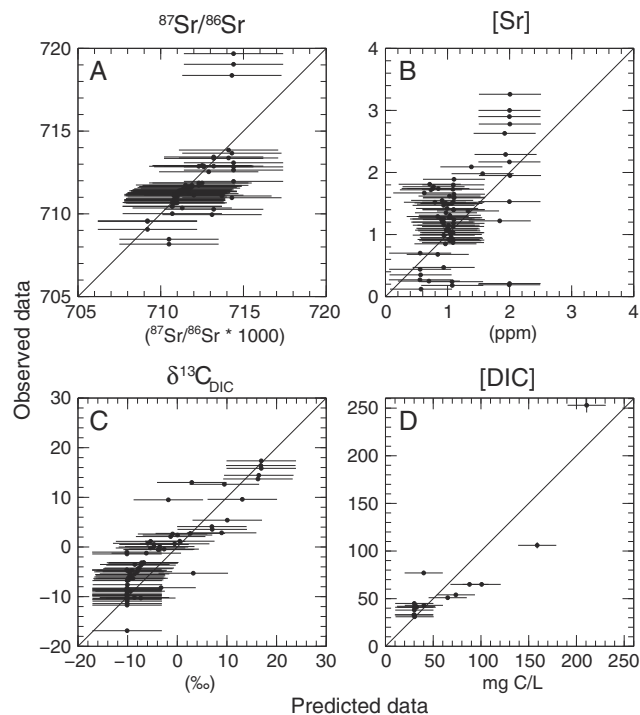


Figure 7. Assessment of model goodness-of-fit. Observed versus predicted (posterior means and 95% credible intervals for replicated data) values for the isotopic and concentration elements. The diagonal line presents the 1:1 line. (a)  $^{87}\text{Sr}/^{86}\text{Sr}$ , (b) [Sr], (c)  $\delta^{13}\text{C}_{\text{DIC}}$  and (d) [DIC]. The three outliers in the  $^{87}\text{Sr}/^{86}\text{Sr}$  (values around 719–720) and [Sr] are from PR02, a sample site on the North Fork of the Powder River that receives input from Cottonwood Creek, which drains a small portion of the Bighorn Mountains. These samples are more radiogenic and have higher [Sr] than any other samples in the study and lie outside of the 95% credible interval for the Archean end member

for example, the CBNG end member's 95% CI for [Sr] contains the means for the Tertiary and carbonate end members, meaning that they are not statistically significantly different from one another. This lack of end-member separation for [Sr] helps to explain the deviation from the 1:1 line (Figure 7b), whereby the model has difficulty determining slight differences between the end members, so most of the data falls into the 1–2 ppm strontium bins. Additionally, the reproducibility for the [Sr] measurements is  $\sim \pm 1$  ppm, which contributes to the 'discretized' appearance of the data. The  $\delta^{13}\text{C}_{\text{DIC}}$  and [DIC] end members are significantly different from one another and do not have overlapping 95% CIs (Table III); hence, the somewhat improved ability of the model to predict the  $\delta^{13}\text{C}_{\text{DIC}}$  and [DIC] data (Figure 7c, d). The end-member results highlight the potential problem of using only [Sr] data in the mixing model framework because the CBNG [Sr] end member is indistinguishable from two of the natural water end members. However, the incorporation of the  $^{87}\text{Sr}/^{86}\text{Sr}$ ,  $\delta^{13}\text{C}_{\text{DIC}}$  and [DIC] data provide clear separation of the end members, which is required in order to estimate their relative contributions to the Powder River.

Model results confirm that both of the tributaries associated with high CBNG activity, Beaver Creek (PR08) and Flying E Creek (PR11) are composed of a significant amount of CBNG produced water (Figure 8). As noted

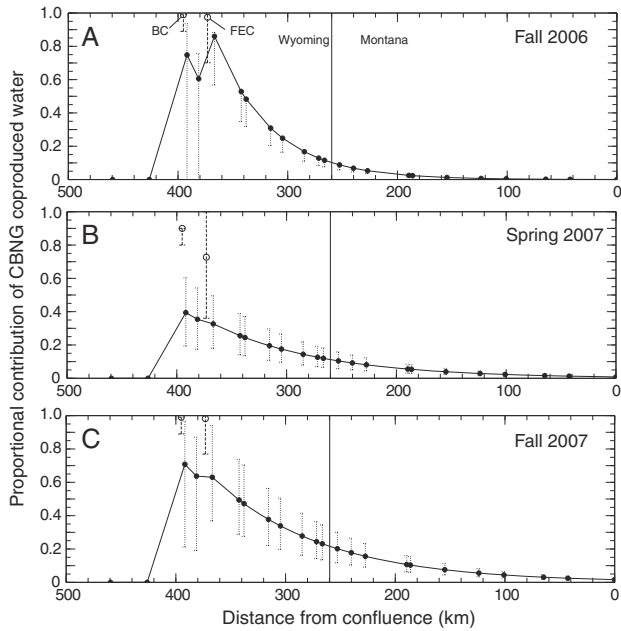


Figure 8. Bayesian estimates (posterior means and 95% credible intervals) of the proportional contribution ( $p_{cbng}$ ) of CBNG produced water in the Powder River plotted versus the distance from the confluence with the Yellowstone River. (a) Low-flow period in fall 2006, (b) high-flow period in spring 2007 and (c) low-flow period in fall 2007. Tributaries are denoted by open symbols (BC = Beaver Creek and FEC = Flying E Creek); Powder River locations are denoted by filled symbols

above, Beaver Creek is dominated by CBNG produced water (WDEQ, 2006), and ~100% of the water in Beaver Creek is CBNG produced water in times of low flow (fall 2006 and 2007) (Figure 8a, c). At times of high flow (spring 2007), the CBNG produced water mixes with spring runoff and comprises ~90% of Beaver Creek (Figure 8b).

Flying E Creek also receives CBNG produced water inputs (WOGCC, 2012). Even though the input volume of CBNG produced water into Flying E Creek is less than that of Beaver Creek, it is still composed mostly of CBNG produced water. That is, the Bayesian mixing model estimated that ~90% of the water in Flying E Creek is derived from CBNG activity at times of low flow (fall 2006 and 2007; Figure 8a, c) and ~70% at times of high flow (spring 2007; Figure 8b).

The Bayesian model estimated that up to 50% of the Powder River is composed of CBNG produced water approximately 20 km downstream of Flying E Creek during times of low flow (Figure 8a, c). The contribution of CBNG produced water decreases as distance from Flying E Creek increases, to an estimated 10–20% proportional contribution at the Montana border during low-flow conditions (Figure 8a, c). In the spring of 2007 (high flow), the model predicts that the Powder River was composed of ~10% CBNG produced water at the Montana border (Figure 8b). These results indicate that CBNG produced water may be a volumetrically significant fraction of the water transported by the Powder River, particularly at times of low flow. The Bayesian mixing model also provided estimates of the relative contributions of the three natural water sources. Only considering the natural

water sources, the relative proportions of these three components were approximately 10% Archean (95% CI=0 - 40%), 45% Tertiary (95% CI=0 - 90%), and 35% carbonate-derived water (95% CI=0 - 70%), although these values were typically poorly resolved as indicated by the 95% CI's.

## DISCUSSION

### Implications of CBNG contributions for Powder River SAR and EC

SAR and EC of the Powder River vary seasonally and with geographic location (Figures 9 and 10, Appendix 2). SAR is calculated using Equation (1), and EC was measured *in situ* by an EC meter. Both SAR and EC are higher under low-flow conditions because there is less melt water, derived from winter snowpack, flowing into the Powder River than there is during the spring when large amounts of dilute melt water greatly increase the discharge of the Powder River and lower the SAR and EC. SAR and EC are at the highest levels in northern Wyoming and in Montana near the confluence with the Yellowstone River (Figures 9 and 10).

We can calculate the EC and SAR values that would result from mixing Powder River water collected upstream of CBNG development with CBNG produced water. If the estimated proportions of CBNG produced water provided by the Bayesian model are accurate, and other processes only have a minimal effect on EC and SAR, then these calculated EC and SAR values should match observed

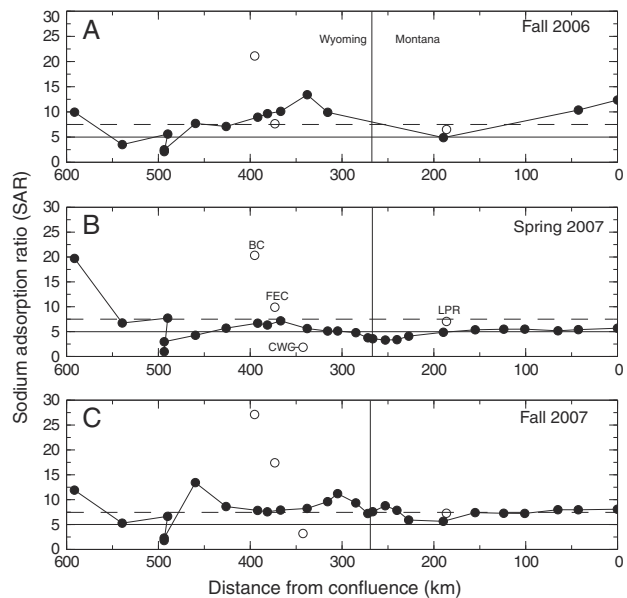


Figure 9. Observed sodium adsorption ratio (SAR) of the Powder River plotted versus distance from the confluence with the Yellowstone River. Horizontal dashed line represents the Montana maximum limit for SAR at the time of sampling (7.5 instantaneous), while the solid line represents the average SAR limit (5). (a) Low-flow period in fall 2006, (b) high-flow period in spring 2007 and (c) low-flow period in fall 2007. Tributaries are denoted by open symbols (BC = Beaver Creek, FEC = Flying E Creek, CWC = Crazy Woman Creek and LPR = Little Powder River); Powder River locations are denoted by filled symbols

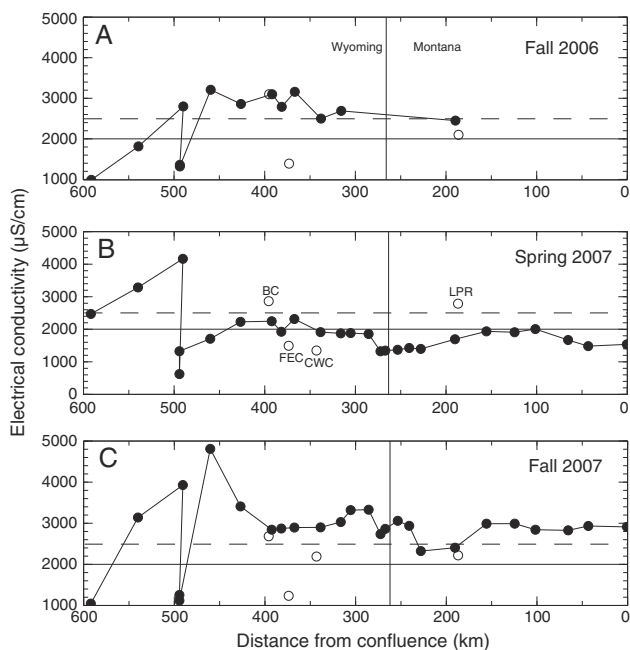


Figure 10. Electrical conductivity (EC) of the Powder River plotted *versus* distance from the confluence with the Yellowstone River. Horizontal dashed line represents the Montana maximum limit for EC at the time of sampling (2500  $\mu\text{S}/\text{cm}$  instantaneous), while the solid line represents the average EC limit (2000  $\mu\text{S}/\text{cm}$ ). Tributaries are denoted by open symbols (BC = Beaver Creek, FEC = Flying E Creek, CWC = Crazy Woman Creek and LPR = Little Powder River); Powder River locations are denoted by filled symbols. (a) Low-flow period in fall 2006, EC samples 29 and 30 are 8800 and 11 190  $\mu\text{S}/\text{cm}$ , respectively, and plot off the scale, (b) high-flow period in spring 2007 and (c) low-flow period in fall 2007

values. These calculations provide an independent method for evaluating the mixing model results. A two end-member mixing model for major ions representative of Powder River water upstream of CBNG production and CBNG produced water (PR08) was implemented in the PHREEQC software, which is available through the USGS. The two water sources were mixed in the model by starting with 100% surface water (0% CBNG water) and incrementally adding 10% of CBNG produced water, up to 100% produced water. A basic regression line for each variable (SAR *vs* percent produced water and EC *vs* percent produced water) was estimated for the PHREEQC mixing results. SAR and EC were computed for the Powder River by plugging in the proportional contribution of CBNG water from Figure 8 into the regression formulas.

The results from the above analysis are plotted as observed *versus* predicted values for SAR and EC (Figure 11). Many of the predicted points for both variables fall below the 1:1 line, indicating that the predicted value is greater than the observed data obtained from the Powder River. This observation reinforces the suggestion from a simple volumetric calculation that the Bayesian model appears to overestimate the proportion of CBNG produced water in the Powder River. This result is not surprising because the Bayesian model assumes that all perturbations of the isotope and ionic concentrations are caused by the influx of CBNG produced water. Within the Bayesian mixing model, we did not allow for other processes that would affect these variables such as evaporation and return

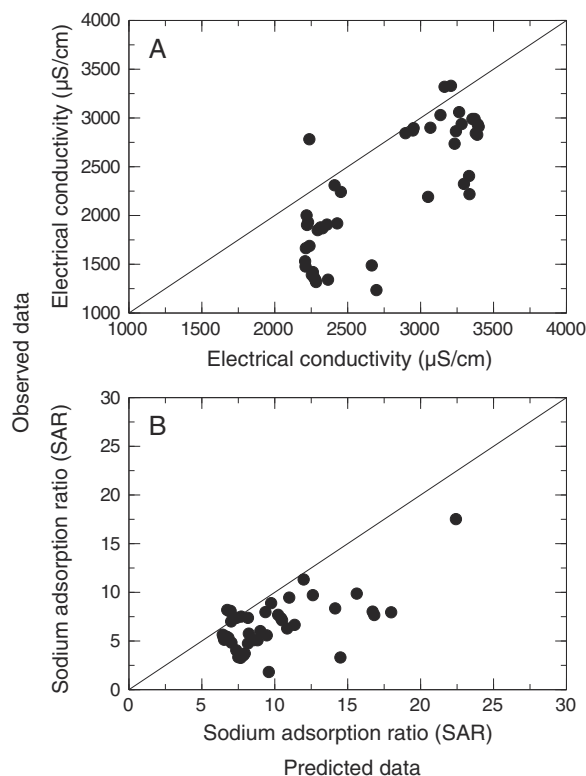


Figure 11. Observed *versus* predicted (obtained from the PHREEQ model) values for SAR and EC based on the Bayesian posterior mean estimates for the proportional contribution of CBNG produced water (from Figure 8) mixing with ‘natural’ Powder River water (based on PR07). (a) EC, and (b) SAR; the diagonal line is the 1:1 line

of irrigated agricultural runoff. The model is an oversimplification of the dynamic Powder River system, but it serves as a robust, yet conservative, upper limit estimate of the proportional contribution of CBNG produced water in the Powder River.

Additionally, there are assumptions in the PHREEQC model (e.g. the use of ‘typical’ Powder River and CBNG water chemistry in the model and not taking into account biological processes that affect water chemistry) that contribute to the oversimplification of the model. The Bayesian mixing model also does not consider water chemistry as it is only based on a linear mixing model that employs mass-balance assumptions. The uncertainty associated with simplifying or neglecting potentially important processes is not directly accounted for in either model. However, such simplifying assumptions are necessary for application of the linear mixing models employed in both the Bayesian mixing model and the PHREEQC model, and we lack sufficient data to inform more complex models. These assumptions do not undercut the credibility of the model, but instead underscore the possibility that other important processes are responsible for the perceived contribution of the CBNG produced water.

Additionally, the potential for the model to overestimate the CBNG produced water contribution to the Powder River emphasizes the fact that there are several interwoven processes that are affecting the Powder River. For example, the Bayesian mixing model estimates suggest a higher proportion of CBNG produced water than would be

expected based upon a simple calculation based on the flows of the CBNG-carrying tributaries and the main stem of the Powder River. For example, during the low-flow sampling event, Beaver Creek contributed  $2 \text{ ft}^3 \text{ s}^{-1}$  of produced water to the Powder River flowing at  $30 \text{ ft}^3 \text{ s}^{-1}$ , representing a contribution of 6.25%. This, along with other evidence discussed below, suggests that the model provides an overestimate of the proportion of CBNG in the Powder River.

*Effect of other processes on SAR and EC of the Powder River*

Inherent in the Montana non-degradation rules is the assumption that the elevated EC and SAR values may be caused by excessive inputs of CBNG produced water. We note that the distance-dependent pattern in the estimated proportion of CBNG produced water (Figure 8) is dissimilar to the pattern in SAR and EC observed from headwaters of the Powder River to its confluence with the Yellowstone River in Montana (Figures 9 and 10). The SAR or EC in northern Wyoming, where CBNG production is focused, vary irregularly and do not appear to correspond to points of discharge of CBNG produced water such as at Beaver Creek and Flying E Creek. Moreover, SAR and EC increase as the Powder River flows northward in Montana. No CBNG production occurs in Montana, which also suggests that the assumption in our model that all perturbation of isotopic and

ionic concentrations are due to CBNG influx is an oversimplification. Thus, we explore the effects of another likely process, evaporation, which can affect SAR and EC.

We evaluated the potential effects of evaporation by implementing another model in PHREEQC that uses typical Powder River water from upstream of CBNG development and instead of mixing the water with CBNG produced water, we evaporated the water in increments of 10%. As the water was evaporated, calcite and aragonite began to precipitate from the water with as little as 10% evaporation using low-flow water chemistry. SAR and EC increased at a rate similar to and often faster than simply mixing produced water with ‘natural’ water (Figure 12). This supports the hypothesis that SAR and EC can be affected by several different processes, with evaporation being a potentially key factor in this semi-arid region, where at low flow the Powder River can form a series of discontinuous pools.

Another process that may be important is irrigation return. This process, although difficult to quantify, may be a factor in Montana where irrigated agriculture is more common than in Wyoming and may be responsible for the increases in SAR and EC along the Montana portion of the Powder River.

We conclude that SAR and EC do not uniquely fingerprint CBNG produced water in the Powder River. On the other hand, environmental tracers, particularly  $\delta^{13}\text{C}_{\text{DIC}}$  in combination with  $^{87}\text{Sr}/^{86}\text{Sr}$  ratios, are effective

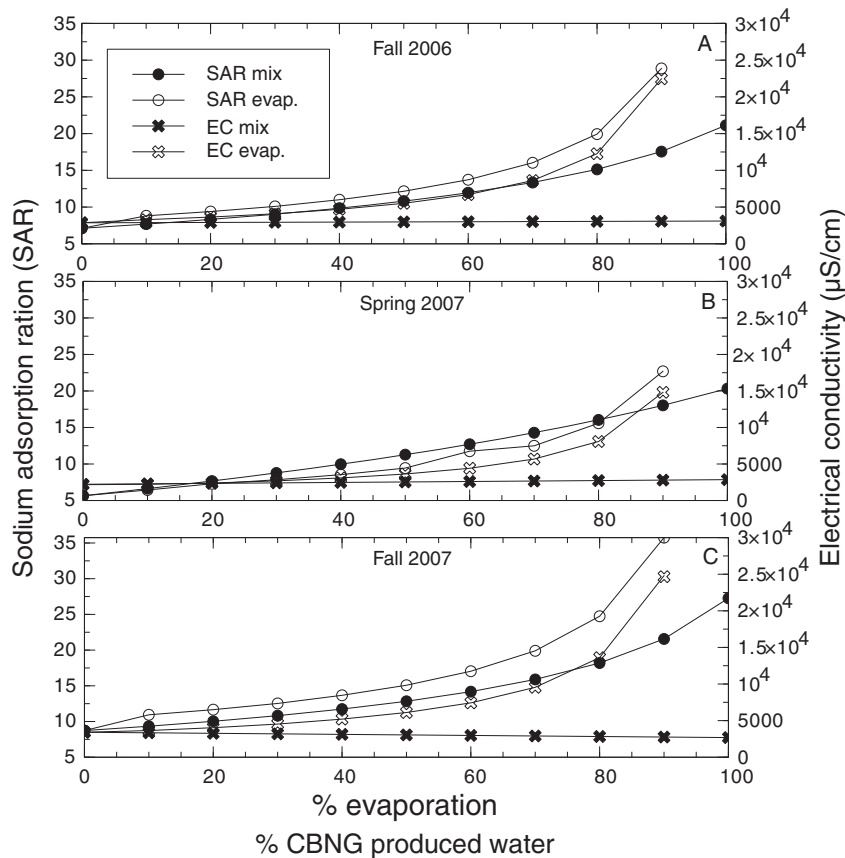


Figure 12. Predicted SAR and EC based on the PHREEQ model *versus* percent contribution of CBNG produced water (black or filled symbols) or percent evaporation (open symbols)

detectors of CBNG produced water. Both tracers applied within the Bayesian framework enabled us to identify a steep decline in the proportion of CBNG produced water as distance from the point sources increases (Figure 8), indicating the Wyoming CBNG produced water likely has little impact on Montana water quality in the Powder River. Other processes, such as evaporation or irrigation return, are likely to be important controls on Powder River water quality.

#### *Dilution of the CBNG signal by input from tributaries*

Although the decay model (Equation (5)) was chosen based on knowledge about real discharge, this exponential model with a single parameter ( $k$ ) creates a smooth decay function that does not easily account for specific major tributary inputs, but accounts for an average of available tributary and main stem discharge data. Between sample locations PR17 and PR18 is the confluence of Clear Creek, which carries approximately the same volume of water as the Powder River. A noticeable drop in EC, SAR and  $\delta^{13}\text{C}_{\text{DIC}}$  between PR17 and PR18 reflects dilution of relatively saline water with high  $\delta^{13}\text{C}_{\text{DIC}}$  that characterizes the Powder River with the low salinity and negative  $\delta^{13}\text{C}_{\text{DIC}}$  water of Clear Creek. The simple decay model that we used does not account for such discrete dilution effects, which could further explain deviations between observed and predicted isotope, concentration, SAR and EC data. However, since a great deal of flow data from tributaries to the Powder River are required, and the complicated seasonal and geographic variations in the hydrology of the PRB make volumetric computations nearly impossible, a more complicated decay function would be difficult to estimate and likely be no more accurate than an exponential decay model, which is supported by Figure 3.

Farther upstream, another tributary with a distinct isotope composition enters the Powder River. PR02 is on the South Fork of the Powder River, and it is just downstream from where another tributary, Cottonwood Creek, joins the river. Cottonwood Creek drains from the Bighorn Mountains and the water at PR02, just downstream of the confluence of Cottonwood Creek and the Powder River, has an elevated  $^{87}\text{Sr}/^{86}\text{Sr}$  ratio ( $\sim 0.719$ ) and [Sr] ( $\sim 3$  ppm) because of high strontium levels contributed by Archean granitic rocks. However, the  $^{87}\text{Sr}/^{86}\text{Sr}$  ratio and [Sr] of PR03, which is  $\sim 50$  km downstream of the confluence with Cottonwood Creek, is quite similar to those values at PR01. This suggests that the volume of water coming in from Cottonwood Creek is very small compared to the overall volume of the Powder River and that the elevated  $^{87}\text{Sr}/^{86}\text{Sr}$  ratio and [Sr] are assimilated into the river, and the Sr isotopic signal is overwhelmed by the comparatively high volume of less radiogenic water brought in by other tributaries to the main stem of the river.

In the case of both PR02 and Clear Creek, the relative input of a tributary could be assessed because of distinctive  $^{87}\text{Sr}/^{86}\text{Sr}$  or  $\delta^{13}\text{C}_{\text{DIC}}$  values compared to the Powder River, identifying locations where the model oversimplifies natural

processes. The PR02 example indicates that the Powder River as a natural system is able to absorb perturbations of fairly small volumes of distinct water, whether it is natural or anthropogenic in nature, with little to no effect on the main stem of the river. The Clear Creek case demonstrates that dilution is a significant factor determining the impact of CBNG produced water on the Powder River. It would be possible to include more detailed information and processes about the hydrology of the PRB into a more detailed Bayesian mixing model, where such information is available. However, the simplified Bayesian mixing model effectively partitions river water sources, and discrepancies between model predictions and observations have highlighted other potentially important factors affecting river chemistry.

## CONCLUSIONS

This study suggests that strontium and carbon isotopes can be used to quantify proportional contributions of different sources of water in a setting where standard geochemical constituents such as major ions,  $\text{Cl}^-$ ,  $\delta^{18}\text{O}$  and  $\delta^2\text{H}$ , fail to uniquely fingerprint these sources. This approach not only applies to the mixing of natural and CBNG produced waters, which have distinctive  $\delta^{13}\text{C}_{\text{DIC}}$ , but also to the mixing of natural sources of water such as the combining of two tributaries with different  $^{87}\text{Sr}/^{86}\text{Sr}$  ratios. The Bayesian statistical model used in this study was able to provide an estimate of the proportional contribution of CBNG produced water in the Powder River, a quantity that eluded previous investigations. Although the model is oversimplified because it neglects processes such as evaporation and agricultural runoff and uses a smooth exponential decay function to account for the dilution of CBNG produced water input, the Bayesian model nevertheless provides a fairly well-constrained upper estimate of the proportion of CBNG produced water in the Powder River.

This study succeeded in part because of the relatively large data set available on strontium and carbon isotopes and concentrations. In many geological studies, there is an inadequate amount of data to parameterize a detailed mixing model. Studies such as this one suggest that collecting sufficient data and using a Bayesian modeling approach for combining such data can account for important sources of uncertainty in the data and process models, accommodate and estimate values for missing data, and quantify the range of potential parameter values (e.g. source contributions) via the posterior distribution. In this study, the Bayesian approach allowed for the simultaneous analysis of strontium and carbon isotopic and concentration data within the context of isotope mixing and mass-balance models. In doing so, we were able to estimate the relative importance of CBNG produced water in the Powder River and infer its importance for water reaching the Montana border.

The estimated proportion of CBNG produced water (10–20%) is expected to have only a minimal effect on the EC and SAR of the Powder River in Montana, and thus current CBNG production rates in Wyoming are not

expected to significantly impact the water quality of the Powder River in Montana. A 20% proportional contribution of CBNG produced water would raise the SAR just 1.3 and 2.0 units for low-flow and high-flow conditions, respectively, and just 0.6 and 1.0 units, respectively, for a 10% proportional contribution. The EC would only be elevated by 25 to 127  $\mu\text{S}/\text{cm}$  for a 10–20% proportional contribution of CBNG produced water at low-flow and high-flow conditions. These potential increases in SAR and EC are not greater than the historic range of measured values for the Powder River prior to CBNG development (Hembree *et al.*, 1953; USGS (2010)). This suggests that current levels of CBNG production are not impacting SAR and EC above historic levels and future regulations regarding SAR and EC in the Powder River should take this into account. Finally, our results demonstrated that addition of CBNG produced water is not the only process that can affect SAR and EC in the Powder River. Evaporation induces changes in EC and SAR of similar or greater magnitude than the addition of current volumes of CBNG produced water in the PRB.

## ACKNOWLEDGEMENTS

We thank M. Meredith and S. Carter for their help in sample collection and S. Sharma and S. Boese for sample analyses. This research is supported by the Department of Energy grant (DE-FC26-06NT155568 – Task 4) to C. Frost administered by the University of Wyoming.

## REFERENCES

- Ayers WB, Jr., Kaiser WR. 1984. Lacustrine-interdeltaic coal in Fort Union Formation (Paleocene), Powder River basin, Wyoming. *AAPG Bulletin*, **68**, 931.
- Brinck EL, Frost CD. 2007. Detecting infiltration and impacts of introduced water using strontium isotopes *Ground Water*, **45**: 554–568.
- Brooks SP, Gelman A. 1998. General methods for monitoring convergence of iterative simulations. *Journal of Computational and Graphical Statistics*, **7**: 434–455.
- Cable J, Ogle K, Tyler AP, Pavao-Zuckerman MA, Huxman TE. 2009. Woody plant encroachment impacts on soil carbon and microbial processes: results from a hierarchical Bayesian analysis of soil incubation data. *Plant and Soil*, **320**: 153–167. DOI: DOI 10.1007/s1104-008-9880-1.
- Cable J, Ogle K, Williams D. 2011. Contribution of glacier meltwater to streamflow in the Wind River Range, Wyoming, inferred via a Bayesian mixing model applied to isotopic measurements. *Hydrological Processes*, **25**: 2228–2236.
- Cable J, Ogle K, Williams DG, Weltzin JF, Huxman TE. 2008. Soil texture drives responses of soil respiration to precipitation pulses in the Sonoran Desert: Implications for climate change. *Ecosystems*, **11**: 961–979. DOI: DOI 10.1007/s10021-008-9172-x.
- Campbell, C. 2007. Strontium Isotopes as Tracers of Water Co-produced with Coal Bed Natural Gas in the Powder River Basin, Wyoming [M.S. Thesis University of Wyoming, 116 p.
- Campbell CE, Pearson BN, Frost CD. 2008. Strontium isotopes as indicators of aquifer communication in an area of coal bed natural gas production, Powder River Basin, Wyoming and Montana. *Rocky Mountain Geology*, **43**: 149–175.
- Carter, SA. 2008. Geochemical Analysis of the Powder River, Wyoming/Montana and an Assessment of the Impacts of Coalbed Natural Gas Co-Produced Water: Laramie, University of Wyoming, p. 147.
- Clark, M.L., Lambing, J.H., Bobst, A.L., 2005. Surface-Water monitoring in watersheds of the Powder River Basin, U.S. Geological Survey Fact Sheet 2005-3137, <http://pubs.usgs.gov/fs/2005/3137/>.
- Clark ML, Mason JP. 2007. Water-quality characteristics for sites in the Tongue, Powder, Cheyenne, and Belle Fourche River drainage basins, Wyoming and Montana, water years 2001–2005, with temporal patterns of selected long-term water-quality data. In: Scientific Investigations Report, Survey USG (ed.), pp: 62 p.
- Crow DW, Mast MA, Bullen TD, Turk JT. 1997. Strontium 87 strontium 86 as a tracer of mineral weathering reactions and calcium sources in an alpine/subalpine watershed, Loch Vale, Colorado. *Water Resources Research*, **33**: 1335–1351.
- Compton, A., 2011, A review of rationale for EC and SAR standards. Helen, MT: Montana Department of Environmental Quality, 44 p. Available at <http://deq.mt.gov/coalbedmethane/finalEIS.mcp>
- DeBruin RH, Lyman RM, Jones RW, Cook LW. 2004. Coalbed methane in Wyoming. In: Information Pamphlet 7 Wyoming State Geological Survey.
- Flores RM, Bader LR. 1999. Fort Union coal in the Powder River Basin, Wyoming and Montana: A synthesis. In: USGS Professional paper 1625-A, 49 p.
- Frost CD, Frost BR, Kirkwood R, Chamberlain KR. 2006. The tonalite-trondhjemite-granodiorite (TTG) to granodiorite-granite (GG) transition in the late Archean plutonic rocks of the central Wyoming Province. *Canadian Journal of Earth Sciences*, **43**: 1419–1444. DOI: Doi 10.1139/E06-082.
- Frost CD, Pearson BN, Ogle KM, Heffern EL, Lyman RM. 2002. Sr isotope tracing of aquifer interactions in an area of accelerating coal-bed methane production, Powder River Basin, Wyoming. *Geology*, **30**: 923–926.
- Frost CD, Toner RN. 2004. Strontium isotopic identification of water-rock interaction and ground water mixing. *Ground Water*, **42**: 418–432.
- Gelman A, Carlin JB, Stern HS, Rubin DB. 2004. Bayesian Data Analysis, 2nd ed. . Chapman & Hall/CRC.
- Gelman A, Hill J. 2006. Data Analysis Using Regression and Multilevel/Hierarchical Models. Cambridge University Press.
- Gelman A, Rubin DB. 1992. Inference from iterative simulation using multiple sequences. *Statistical Science*, **7**: 457–511.
- Gilks WR, Richardson S, Spiegelhalter DJ. 1996. Markov Chain Monte Carlo in Practice. Chapman & Hall/CRC.
- Hembree CH, Colby BR, Swenson HA, Davis JR. 1953. Sedimentation and Chemical Quality of Water in the Powder River Drainage Basin Wyoming and Montana. *USGS Circular* **170**: 92.
- Hinaman KC. 2005. Hydrogeologic Framework and Estimates of Ground-Water Volumes in Tertiary and Upper Cretaceous Hydrologic Units in the Powder River Basin, Wyoming. In: <http://pubs.usgs.gov/sir/2005/5008/>, USGS, 18 p.
- Hong BG, Strawderman RL, Swaney DP, Weinstein DA. 2005. Bayesian estimation of input parameters of a nitrogen cycle model applied to a forested reference watershed, Hubbard Brook Watershed Six. *Water Resources Research*, **41**: W03007. DOI: 10.1029/2004WR003551
- Hotchkiss WR, Levings JF. 1986. Hydrogeology and simulation of water flow in strata above the Bearpaw Shale and equivalents of eastern Montana and northeastern Wyoming. U.S. Geological Survey Water-Resources Investigations Report 85–4281: 72.
- Lunn DJ, Thomas A, Best N, Spiegelhalter D. 2000. WinBUGS - A Bayesian modelling framework: Concepts, structure, and extensibility. *Statistics and Computing*, **10**: 325–337.
- Montana Department of Environmental quality (MDEQ), 2006, Numeric Standards for Electrical Conductivity (EC) and Sodium Adsorption Ratio (SAR), Volume 17.30.670
- Mook WG, Tan FC. 1991. Stable carbon isotopes in rivers and estuaries. In: *Biogeochemistry of Major World Rivers*, Degens ET, Kempe S, Richey JE (eds.) John Wiley and Sons: Chichester.
- Moore JW, Semmens BX. 2008. Incorporating uncertainty and prior information into stable isotope mixing models. *Ecology Letters*, **11**: 470–480. DOI: 10.1111/j.1461-0248.2008.01163.x.
- Ogle K, Barber JJ. 2008. Bayesian data-model integration in plant physiological and ecosystem ecology. *Progress in Botany*, **69**: 281–311.
- Ogle K, Uriarte M, Thompson J, Johnstone J, Jones A, Lin Y, McIntire E, Zimmerman J. 2006. Implications of vulnerability to hurricane damage for long-term survival of tropical tree species: A Bayesian hierarchical analysis. In: *Hierarchical Modeling for the Environmental Sciences: Statistical Methods and Applications*, Clark JS, Gelfand AE (eds.) Oxford University Press: Oxford.
- Ogle K, Wolpert RL, Reynolds JF. 2004. Reconstructing plant root area and water uptake profiles. *Ecology*, **85**: 1967–1978.
- Parnell AC, Inger R, Bearhop S, Jackson AL. 2010. Source partitioning using stable isotopes: Coping with too much variation. *PLoS One*, **5**: e9672.
- Payne AA, Saffer DM. 2005. Surface water hydrology and shallow groundwater effects of coalbed natural gas development, upper Beaver Creek drainage, Powder River Basin, Wyoming. In: *Western resources*

- project final report – produced groundwater associated with coalbed natural gas production in the Powder River Basin, Zoback MD (ed.) Wyoming State Geological Survey: Laramie, Wyoming.*
- Pearson, BN. 2002. Sr Isotope Ratio as a Monitor of Recharge and Aquifer Communication, Paleocene Fort Union Formation and Eocene Wasatch Formation, Powder River Basin, Wyoming and Montana [M.S. Thesis: University of Wyoming.
- Pennaco. 2009. Pennaco Energy Company, Inc. vs. Bureau of Land Management, Volume 06cv100, U.S. District Court for the District of Wyoming.
- Quillinan, SA, Frost, C. D., 2012. Spatial variability of coalbed natural gas produced water quality, Powder River basin: Implications for future development: Wyoming State Geological Survey Report of Investigation: No. 64, 58 pp.
- Sharma S, Frost CD. 2008. Tracing coalbed natural gas-coproducted water using stable isotopes of carbon. *Ground Water*, **46**: 329–334. DOI: 10.1111/j.1745-6584.2007.00417.x.
- Sharp WN, Gibbons AB. 1964. Geology and uranium deposits of the southern part of the Powder River Basin, Wyoming. U. S. Geological Survey Bulletin, Report: B 1147-D: D1-D60.
- Stumm W, Morgan JJ. 1996. *Aquatic chemistry: Chemical equilibria and rates in natural waters, 3d ed. John Wiley and Sons, Inc.*
- United States Geological Survey (USGS) National Water Information System. USGS Water Data for the Nation. <http://waterdata.usgs.gov/nwis>. 2010.
- United States Geological Survey (USGS). 2005. Surface-Water monitoring in watersheds of the Powder River Basin. In: Powder River Basin Interagency Working Group.
- Wang X, Melesse AM, McClain ME, Yang W. 2007. Water quality changes as a result of coalbed methane development in a Rocky Mountain watershed. *Journal of the American Water Resources Association*, **43**: 1383–1399.
- Wheaton J, Brown TH. 2005. Predicting changes in groundwater quality associated with coalbed natural gas infiltration ponds. In: *Western resources project final report – produced groundwater associated with coalbed natural gas production in the Powder River Basin, Zoback MD (ed.) Wyoming State Geological Survey: Laramie, Wyoming.*
- Whiticar MJ. 1999. Carbon and hydrogen isotope systematics of bacterial formation and oxidation of methane. *Chemical Geology*, **161**: 291–314.
- Wyoming Department of Environmental Quality (WDEQ), 2006. WYPDES program WY0046922.
- Wyoming Department of Environmental Quality (WDEQ). 2008. WYPDES program WY0053066.
- Wyoming Oil and Gas Conservation Commission (WOGCC). 2012. <http://wogcc.state.wy.us/coalbedchart.cfm>.

## APPENDIX I. WINBUGS CODE

## Model

```
{
# First, we create a j loop for the three field seasons. Next, we loop through samples 1–3
# to determine the Archean aka granitic type water end member which does not vary by
# season; .rep creates replicated data to test observed versus predicted values for the
# model

for (j in 1:3){
  for (i in 1:3){
    # Define likelihoods of observed end-member data and create replicated data.
    SrRatio[i,j] ~ dnorm(SrR.arc, tau.SrR)
    SrRatio.rep[i, j] ~ dnorm(SrR.arc, tau.SrR)

    Sr[i,j] ~ dnorm(Sr.arc, tau.Sr)
    Sr.rep[i,j] ~ dnorm(Sr.arc, tau.Sr)
  }
# the i loop is closed. and we move on to defining the other end members, carbonate
# and tertiary sediments; these end members will also vary by season and are
# defined by the field data

#PR04 is used to define the carbonate water end member. Likelihood for these data:
SrRatio[4,j] ~ dnorm(SrR.carb, tau.SrR)
SrRatio.rep[4,j] ~ dnorm(SrR.carb, tau.SrR)

Sr[4,j] ~ dnorm(Sr.carb, tau.Sr)
Sr.rep[4,j] ~ dnorm(Sr.carb, tau.Sr)

#PR05 is used to determine the tertiary end member. Likelihood for these data:
SrRatio[5,j] ~ dnorm(SrR.tert, tau.SrR)
SrRatio.rep[5,j] ~ dnorm(SrR.tert, tau.SrR)

Sr[5,j] ~ dnorm(Sr.tert, tau.Sr)
Sr.rep[5,j] ~ dnorm(Sr.tert, tau.Sr)

#PR01-05 define the ‘natural’ end member for the DIC data, with likelihoods:
for (i in 1:5){
  d13C[i,j] ~ dnorm(d13C.nw, tau.d13C)
  d13C.rep[i,j] ~ dnorm(d13C.nw, tau.d13C)
}
```

```

C[i,j] ~ dnorm(C.nw, tau.C)
C.rep[i,j] ~ dnorm(C.nw, tau.C)
}

```

```

#PR06 and PR07 are sites after the confluence of the three forks, but before Beaver Creek
# enters. A mixing model is employed to determine the contribution of each fork using
# strontium isotopes and concentration. The likelihoods for these stations are:

```

```

SrRatio[6,j] ~ dnorm(mu.SrRatio.conf6[6,j], tau.SrR)
SrRatio.rep[6,j] ~ dnorm(mu.SrRatio.conf6[6,j], tau.SrR)

```

```

SrRatio[7,j] ~ dnorm(mu.SrRatio.conf7[7,j], tau.Sr)
SrRatio.rep[7,j] ~ dnorm(mu.SrRatio.conf7[7,j], tau.Sr)

```

```

d13C[6,j] ~ dnorm(mu.d13C.conf6[6,j], tau.d13C)
d13C.rep[6,j] ~ dnorm(mu.d13C.conf6[6,j], tau.d13C)

```

```

d13C[7,j] ~ dnorm(mu.d13C.conf7[7,j], tau.d13C)
d13C.rep[7,j] ~ dnorm(mu.d13C.conf7[7,j], tau.d13C)

```

```

Sr[6,j] ~ dnorm(mu.Sr.conf6[j], tau.Sr)
Sr.rep[6,j] ~ dnorm(mu.Sr.conf6[j], tau.Sr)

```

```

Sr[7,j] ~ dnorm(mu.Sr.conf7[j], tau.Sr)
Sr.rep[7,j] ~ dnorm(mu.Sr.conf7[j], tau.Sr)

```

```

C[6,j] ~ dnorm(mu.C.conf6[j], tau.C)
C.rep[6,j] ~ dnorm(mu.C.conf6[j], tau.C)

```

```

C[7,j] ~ dnorm(mu.C.conf7[j], tau.C)
C.rep[7,j] ~ dnorm(mu.C.conf7[j], tau.C)

```

```

# Define mixing model (means) for these stations:

```

```

mu.SrRatio.conf6[6,j] <- p6.arc[j]*cut.SrR.arc + p6.carb[j]*cut.SrR.carb + p6.tert[j]*cut.SrR.tert
mu.SrRatio.conf7[7,j] <- p7.arc[j]*cut.SrR.arc + p7.carb[j]*cut.SrR.carb + p7.tert[j]*cut.SrR.tert

```

```

mu.d13C.conf6[6,j] <- p6.arc[j]*cut.d13C.nw + p6.carb[j]*cut.d13C.nw +
p6.tert[j]*cut.d13C.nw
mu.d13C.conf7[7,j] <- p7.arc[j]*cut.d13C.nw + p7.carb[j]*cut.d13C.nw +
p7.tert[j]*cut.d13C.nw

```

```

mu.Sr.conf6[j] <- p6.arc[j]*cut.Sr.arc + p6.carb[j]*cut.Sr.carb + p6.tert[j]*cut.Sr.tert
mu.C.conf6[j] <- p6.arc[j]*cut.C.nw + p6.carb[j]*cut.C.nw + p6.tert[j]*cut.C.nw

```

```

mu.Sr.conf7[j] <- p7.arc[j]*cut.Sr.arc + p7.carb[j]*cut.Sr.carb + p7.tert[j]*cut.Sr.tert
mu.C.conf7[j] <- p7.arc[j]*cut.C.nw + p7.carb[j]*cut.C.nw + p7.tert[j]*cut.C.nw

```

```

# Cumulative logits model for the relative contributions for locations PR06 and PR07:

```

```

w6[j] <- 1 + exp(u6.arc[j]) + exp(u6.carb[j])
p6.arc[j] <- exp(u6.arc[j])/w6[j]
p6.carb[j] <- exp(u6.carb[j])/w6[j]
p6.tert[j] <- 1 - p6.arc[j] - p6.carb[j]

```

```

w7[j] <- 1 + exp(u7.arc[j]) + exp(u7.carb[j])
p7.arc[j] <- exp(u7.arc[j])/w7[j]
p7.carb[j] <- exp(u7.carb[j])/w7[j]
p7.tert[j] <- 1 - p7.arc[j] - p7.carb[j]

```

```

# Assign normal, hierarchical priors to the logit-scale parameters:

```

```

u6.arc[j] ~ dnorm(mu6.u.arc, tau.arc)
u6.carb[j] ~ dnorm(mu6.u.carb, tau.carb)

```

```

u7.arc[j] ~ dnorm(mu7.u.arc, tau.arc)
u7.carb[j] ~ dnorm(mu7.u.carb, tau.carb)

```

# Now, we move on to the rest of the PR sites. Define the CBNG end member based  
 # on Beaver Creek (station 8). Likelihoods for this station's data:  
 $SrRatio[8,j] \sim dnorm(SrR.cbm, \tau.SrR)$   
 $SrRatio.rep[8,j] \sim dnorm(SrR.cbm, \tau.SrR)$

$Sr[8,j] \sim dnorm(Sr.cbm, \tau.Sr)$   
 $Sr.rep[8,j] \sim dnorm(Sr.cbm, \tau.Sr)$

$d13C[8,j] \sim dnorm(d13C.cbm, \tau.d13C)$   
 $d13C.rep[8,j] \sim dnorm(d13C.cbm, \tau.d13C)$

$C[8,j] \sim dnorm(C.cbm, \tau.C)$   
 $C.rep[8,j] \sim dnorm(C.cbm, \tau.C)$

# Now, we can loop through the remaining stations, which are characterized  
 # as a mixture of natural waters and CBNG water.

for (i in 9:30){  
 # Define likelihoods for data at each of these stations:  
 $SrRatio[i,j] \sim dnorm(\mu.SrR[i-8,j], \tau.SrR)$   
 $SrRatio.rep[i,j] \sim dnorm(\mu.SrR[i-8,j], \tau.SrR)$

$d13C[i,j] \sim dnorm(\mu.d13C[i-8,j], \tau.d13C)$   
 $d13C.rep[i,j] \sim dnorm(\mu.d13C[i-8,j], \tau.d13C)$

$Sr[i,j] \sim dnorm(\mu.Sr[i-8,j], \tau.Sr)$   
 $Sr.rep[i,j] \sim dnorm(\mu.Sr[i-8,j], \tau.Sr)$

$C[i,j] \sim dnorm(\mu.C[i-8,j], \tau.C)$   
 $C.rep[i,j] \sim dnorm(\mu.C[i-8,j], \tau.C)$

# Define mixing models (means):

$\mu.SrR[i-8,j] <- p.cbm[i-8,j]*cut.SrR.cbm + p.arc[i-8,j]*cut.SrR.arc +$   
 $p.carb[i-8,j]*cut.SrR.carb + p.tert[i-8,j]*cut.SrR.tert$

$\mu.d13C[i-8,j] <- p.cbm[i-8,j]*cut.d13C.cbm + p.arc[i-8,j]*cut.d13C.nw +$   
 $p.carb[i-8,j]*cut.d13C.nw + p.tert[i-8,j]*cut.d13C.nw$

$\mu.Sr[i-8,j] <- p.cbm[i-8,j]*cut.Sr.cbm + p.arc[i-8,j]*cut.Sr.arc +$   
 $p.carb[i-8,j]*cut.Sr.carb + p.tert[i-8,j]*cut.Sr.tert$

$\mu.C[i-8,j] <- p.cbm[i-8,j]*cut.C.cbm + p.arc[i-8,j]*cut.C.nw +$   
 $p.carb[i-8,j]*cut.C.nw + p.tert[i-8,j]*cut.C.nw$

# Define the CBNG contribution(p.cbm) via the exponential decay model:

$A[i-8,j] <- p0.cbm[j]*exp(-k[j]*Distance1[i])$

$B[i-8,j] <- p1.cbm[j]*exp(-k[j]*Distance2[i])$

$p.cbm[i-8,j] <- A[i-8,j]*step(10.5-i) + p0.cbm11[j]*equals(i,11) +$   
 $(A[i-8,j] + B[i-8,j])*(1-(step(11.5-i)))$

# Cumulative logits model for the natural water contributions:

$w[i-8,j] <- 1 + exp(u.arc[i-8,j]) + exp(u.carb[i-8,j])$

$q.arc[i-8,j] <- exp(u.arc[i-8,j])/w[i-8,j]$

$q.carb[i-8,j] <- exp(u.carb[i-8,j])/w[i-8,j]$

$q.tert[i-8,j] <- 1 - q.arc[i-8,j] - q.carb[i-8,j]$

$p.arc[i-8,j] <- (1-p.cbm[i-8,j])*q.arc[i-8,j]$

$p.tert[i-8,j] <- (1-p.cbm[i-8,j])*q.tert[i-8,j]$

$p.carb[i-8,j] <- (1-p.cbm[i-8,j])*q.carb[i-8,j]$

$p.carb.tert[i-8,j] <- p.tert[i-8,j] + p.carb[i-8,j]$

$p.nw.all[i-8,j] <- p.tert[i-8,j] + p.carb[i-8,j] + p.arc[i-8,j]$

# Assign normal, hierarchical prior to the logit-scale parameter:

```

u.arc[i-8,j] ~ dnorm(mu.u.arc, tau.arc)
u.carb[i-8,j] ~ dnorm(mu.u.carb, tau.carb)
}
# Assign non-informative, uniform prior to decay parameter:
k[j] ~ dunif(0,1)

# Assign non-informative priors to the initial CBNG contributions in the
# Beaver Creek and Flying E creek:
p0.cbm[j] <- - exp(u0.cbm[j])/(1 + exp(u0.cbm[j]))
u0.cbm[j] ~ dnorm(0,0.001)

p1.cbm.dummy[j] <- -exp(u1.cbm.dummy[j])/(1 + exp(u1.cbm.dummy[j]))
u1.cbm.dummy[j] ~ dnorm(0,0.001)

Astar[j] <- (1-A[3,j])
p1.cbm[j] <- -p1.cbm.dummy[j]*Astar[j]

p0.cbm11[j] <- - exp(u0.cbm11[j])/(1 + exp(u0.cbm11[j]))
u0.cbm11[j] ~ dnorm(0,0.001)
}
# Assign semi-informative priors to end-member values, and use the 'cut' values
# in the above mixing models to avoid feedback between the mixture data and the
# end-member estimates:

SrR.arc ~ dnorm(713,1)
cut.SrR.arc <- - cut(SrR.arc)

Sr.arc ~ dnorm(2.0, 0.1)
cut.Sr.arc <- - cut(Sr.arc)

SrR.carb ~ dnorm(709, 1)
cut.SrR.carb <- - cut(SrR.carb)

Sr.carb ~ dnorm(0.5, 0.1)
cut.Sr.carb <- - cut(Sr.carb)

SrR.tert ~ dnorm(711, 1)
cut.SrR.tert <- - cut(SrR.tert)

Sr.tert ~ dnorm(1.0, 0.1)
cut.Sr.tert <- - cut(Sr.tert)

Sr.cbm ~ dnorm(0.5, 0.1)I(0,)
cut.Sr.cbm <- - cut(Sr.cbm)

SrR.cbm ~ dnorm(713.2, 0.1)
cut.SrR.cbm <- - cut(SrR.cbm)

d13C.nw ~ dnorm(-10,0.1)
cut.d13C.nw <- - cut(d13C.nw)

C.nw ~ dnorm(30, 0.1)
cut.C.nw <- - cut(C.nw)

d13C.cbm ~ dnorm(17.5, 0.1)
cut.d13C.cbm <- - cut(d13C.cbm)

C.cbm ~ dnorm(150, 0.001)
cut.C.cbm <- - cut(C.cbm)

# Assign non-informative priors to remaining parameters (e.g. global mean
# proportions on the logit scale and precision terms):

mu6.u.arc ~ dnorm(0.0,0.001)
mu6.u.carb ~ dnorm(0.0,0.001)

```

```

mu7.u.arc ~ dnorm(0.0,0.001)
mu7.u.carb ~ dnorm(0.0,0.001)

mu.u.arc ~ dnorm(0.0,0.001)
mu.u.carb ~ dnorm(0.0,0.001)

tau.arc ~ dgamma(0.1,0.1)
tau.carb ~ dgamma(0.1,0.1)

tau.SrR ~ dgamma(0.1,0.1)
tau.Sr ~ dgamma(0.1,0.1)

tau.d13C ~ dgamma(0.1,0.1)
tau.C ~ dgamma(0.1,0.1)
}

```

#Initial values used for three MCMC chains

```
list(mu.u.arc = 14, mu.u.carb = 15, tau.arc = 4, tau.carb = 8, tau.SrR = .5, tau.Sr = 2.5, mu6.u.arc = 10, mu6.u.carb = 10, mu7.u.arc = 10, mu7.u.carb = 10, tau.d13C = .5, tau.C = 2.5)
```

```
list(mu.u.arc = 10, mu.u.carb = 20, tau.arc = 10, tau.carb = 5, tau.SrR = 1, tau.Sr = 5, mu6.u.arc = 15, mu6.u.carb = 1, mu7.u.arc = .5, mu7.u.carb = 1, tau.d13C = 1, tau.C = 5)
```

```
list(mu.u.arc = 20, mu.u.carb = 10, tau.arc = 1, tau.carb = 10, tau.SrR = 2, tau.Sr = 1, mu6.u.arc = 2, mu6.u.carb = 15, mu7.u.arc = 2, mu7.u.carb = .1,
```

## APPENDIX II. EC AND SAR DATA

Sample Site	Fall 2006 EC (µS/cm)	SAR	Spring 2007 EC (µS/cm)	SAR	Fall 2007 EC (µS/cm)	SAR
PR 01	990	9.95	2466	19.68	1046	12.03
PR 02	1815	3.51	3280	6.70	3140	5.39
PR 03	2800	5.60	4160	7.68	3930	6.76
PR 04	1360	2.11	618	0.94	1256	1.90
PR 05	1320	2.49	1320	2.93	1120	2.40
PR 06	3210	7.71	1703	4.23	4810	13.54
PR 07	2860	7.11	2223	5.66	3410	8.73
PR 08 <sup>a</sup>	NA	21.11	2858	20.30	2684	27.23
PR 09	3100	8.95	2242	6.66	2844	7.95
PR 10	2790	9.65	1919	6.29	2872	7.67
PR 11 <sup>a</sup>	1390	7.65	1488	9.87	1235	17.52
PR 12	3160	10.11	2310	7.13	2896	8.02
PR 13 <sup>a</sup>	NA	NA	1342	1.82	2191	3.31
PR 14	2500	13.41	1907	5.58	2900	8.35
PR 15	2690	9.92	1839	5.08	3030	9.71
PR 16	NA	NA	1878	5.09	3320	11.32
PR 17	NA	NA	1850	4.75	3330	9.46
PR 18	NA	NA	1318	3.72	2736	7.33
PR 19	NA	NA	1339	3.53	2864	7.69
PR 20	NA	NA	1365	3.27	3060	8.89
PR 21	NA	NA	1420	3.34	2938	7.97
PR 22	NA	NA	1391	4.05	2324	6.02
PR 23	2450	4.89	1688	4.83	2405	5.76
PR 24 <sup>a</sup>	2100	6.51	2782	7.01	2219	7.38
PR 25	NA	NA	1931	5.33	2990	7.51
PR 26	NA	NA	1903	5.45	2990	7.38
PR 27	NA	NA	2001	5.46	2843	7.35
PR 28	NA	NA	1665	5.13	2828	8.09
PR 29	8890	10.37	1477	5.36	2934	8.08
PR 30	11190	12.36	1531	5.65	2911	8.19

